



저작자표시-비영리-변경금지 2.0 대한민국

이용자는 아래의 조건을 따르는 경우에 한하여 자유롭게

- 이 저작물을 복제, 배포, 전송, 전시, 공연 및 방송할 수 있습니다.

다음과 같은 조건을 따라야 합니다:



저작자표시. 귀하는 원저작자를 표시하여야 합니다.



비영리. 귀하는 이 저작물을 영리 목적으로 이용할 수 없습니다.



변경금지. 귀하는 이 저작물을 개작, 변형 또는 가공할 수 없습니다.

- 귀하는, 이 저작물의 재이용이나 배포의 경우, 이 저작물에 적용된 이용허락조건을 명확하게 나타내어야 합니다.
- 저작권자로부터 별도의 허가를 받으면 이러한 조건들은 적용되지 않습니다.

저작권법에 따른 이용자의 권리는 위의 내용에 의하여 영향을 받지 않습니다.

이것은 [이용허락규약\(Legal Code\)](#)을 이해하기 쉽게 요약한 것입니다.

[Disclaimer](#)

이학석사학위논문

자연 발생 이소프렌 배출이 서울
지역 오존 대기질에 미치는 영향

Impacts of biogenic isoprene emission on
ozone air quality in the Seoul metropolitan
area

2013년 7월

서울대학교 대학원

지구환경과학부

이 광 연

자연 발생 이소프렌 배출이 서울
지역 오존 대기질에 미치는 영향
Impacts of biogenic isoprene emission on
ozone air quality in the Seoul metropolitan
area

지도교수 백 종 진

이 논문을 이학석사 학위논문으로 제출함

2013년 6월

서울대학교 대학원

지구환경과학부

이 광 연

이광연의 이학석사 학위논문을 인준함

2013년 7월

위 원 장 _____ (인)

부위원장 _____ (인)

위 원 _____ (인)

Abstract

The impacts of biogenic isoprene emission on ozone air quality and the effect of interaction between biogenic isoprene emission and urban breeze circulation on ozone air quality during an episode of weak synoptic forcing in the Seoul metropolitan area, South Korea, are investigated using WRF model coupled with Seoul National University Urban Canopy Model and CMAQ model. The biogenic isoprene emission increases daily maximum ozone concentration by 37 ppb in the urban area. The biogenic isoprene emitted from the surrounding region of Seoul has larger impacts on the ozone concentration in the urban area than the biogenic isoprene emitted from the Seoul region. The gas-phase chemistry is the most important process to the ozone concentration in the daytime when the urban breeze circulation is well developed in the presence of the biogenic isoprene emission. The lifetime of isoprene is not long enough (around 30 minutes) to directly affect ozone concentration in the urban area. Rather than isoprene, MA_PAN which is produced from isoprene by gas-phase chemistry links the biogenic isoprene emitted from the surrounding region and ozone in the urban area. MA_PAN produced in the surrounding area is transported into the urban area and dissociate into other species which produce ozone in

the urban area. Urban breeze circulation is an important atmospheric phenomenon that affects ozone concentration in the urban area. When the urban and industrial surfaces are artificially replaced with the cropland surface, urban breeze circulation is not well developed. In this case, the ozone concentration generally decreases by about 10% and the contribution of gas-phase chemistry to the ozone concentration is decreased in the urban area. It is caused by the decrement of transport of the ozone precursor from the surrounding area to the urban area. The results from this study can be give some insight about how biogenic isoprene affect the ozone concentration in the urban area.

Key Words : Biogenic isoprene emission, Ozone air quality, Urban area, Urban breeze circulation, WRF model, CMAQ model

Student's number : 2011-23267

Contents

Abstract	i
Contents	iii
List of Figures	v
List of Tables	xi
1. Introduction	1
2. Methodology	4
2.1 Meteorology modeling system.....	4
2.2 Air quality modeling system.....	5
2.3 Simulation scenarios.....	7
3. Results and discussion	11
3.1 Model validation.....	11
3.2 Impacts of biogenic isoprene emission.....	14
3.3 Effect of interaction between biogenic isoprene emission and urban breeze circulation.....	37
4. Summary and conclusions	48
References	52

초록..... 59

List of Figures

Figure 1. (a) CMAQ simulation domains with terrain height and (b) land-use/land-cover in the innermost domain. The white circles indicate air quality monitoring sites, and the blue line indicates the location of vertical cross section that is shown in Figs. 10 and 11. The isoprene emission rate in the (c) ALL, (d) NONE, (e) OUT, and (f) IN simulations at 15 LT 24 June 2010 in the innermost domain.9

Figure 2. (a) Diurnal variations of observed and simulated ozone concentration near the surface on 24 June 2010. The dots and shading indicate the observed ozone concentration at air quality monitoring sites and the simulated ozone concentration at the corresponding grids in the innermost domain, respectively. The black and grey lines indicate the average ozone concentration of observation and simulation, respectively. (b) Scatter plot of observed ozone concentration versus simulated ozone concentration on 24 June 2010. The unit of MNBE and MNGE is %, and the unit of MBE and RMSE is ppb.12

Figure 3. Diurnal variations of atmospheric boundary layer averaged

concentrations of (a) ozone and (c) isoprene in the ALL, OUT, IN, and NONE simulations in the urban area. (b) Diurnal variations of ozone concentration differences between the ALL simulation and the OUT, IN, or NONE simulation in the urban area.....16

Figure 4. Horizontal distributions of atmospheric boundary layer averaged ozone concentrations in the (a) ALL, (b) NONE, (c) OUT, and (d) IN simulations, and the ratio of the ozone concentration differences between the ALL simulation and the (e) OUT or (f) IN simulation to the ozone concentration in the ALL simulation at 15 LT. Horizontal wind fields are at the lowest model level.19

Figure 5. Diurnal variations of atmospheric boundary layer averaged contributions of individual processes to the ozone concentration from 06 to 20 LT in the (a) ALL, (b) NONE, (c) OUT, and (d) IN simulations in the urban area.....22

Figure 6. 5-hour averaged vertical profiles of contributions of individual processes to the ozone concentration averaged over the urban area for the period from 11 to 15 LT in the (a) ALL, (b) NONE, (c) OUT, and (d) IN simulations.....24

Figure 7. (a) Diurnal variations of atmospheric boundary layer averaged HCHO concentration in the ALL, OUT, IN, and NONE simulations. (b) Diurnal variations of HCHO concentration difference between the ALL simulation and OUT, IN, or NONE simulation in the urban area. Diurnal variations of atmospheric boundary layer averaged contributions of individual processes to the HCHO concentration from 06 to 20 LT in the (c) ALL, (d) NONE, (e) OUT, and (f) IN simulations in the urban area.....26

Figure 8. (a) Diurnal variations of atmospheric boundary layer averaged MA_PAN concentration in the ALL, OUT, IN, and NONE simulations in the urban area. (b) Diurnal variations of atmospheric boundary layer averaged MA_PAN concentration differences between the ALL simulation and the OUT, IN, or NONE simulation in the urban area. Diurnal variations of atmospheric boundary layer averaged contributions of individual processes to the MA_PAN concentration from 06 to 20 LT in the (c) ALL, (d) NONE, (e) OUT, and (f) IN simulations in the urban area.....30

Figure 9. 5-hour averaged vertical profiles of (a) MA_PAN

concentrations in the ALL, OUT, IN, and NONE simulations, and contributions of individual processes to the MA_PAN concentration in the (b) ALL, (c) NONE, (d) OUT, and (e) IN simulations in the urban area.....33

Figure 10. Vertical cross sections of contribution of transport to the MA_PAN concentration in the (a) ALL, (c) OUT, and (e) IN simulations at 17 LT. Vertical cross sections of contribution of chemical reaction to the MA_PAN concentration in the (b) ALL, (d) OUT, and (f) IN simulations at 17 LT.....35

Figure 11. Vertical cross sections of ozone concentration in the (a) ALL, (c) OUT, and (e) IN simulations at 17 LT. Vertical cross sections of contribution of chemical reaction to the ozone concentration in the (b) ALL, (d) OUT, and (f) IN simulations at 17 LT.....36

Figure 12. Diurnal variations of atmospheric boundary layer averaged concentrations of (a) ozone, (c) isoprene in the NOURB-ALL, NOURB-OUT, NOURB-IN, and NOURB-NONE simulations. (b) Diurnal variations of atmospheric boundary layer averaged ozone

concentration differences between NOURB-ALL simulation and NOURB-OUT, NOURB-IN, or NOURB-NONE simulation in the urban area. (d) Diurnal variations of atmospheric boundary layer averaged ozone concentration differences between the URB-type simulations and NOURB-type simulations.....39

Figure 13. Diurnal variations of atmospheric boundary layer averaged contributions of individual processes to ozone concentration in the (a) NOURB-ALL, (b) NOURB-NONE, (c) NOURB-OUT, and (d) NOURB-IN simulations in the urban area from 06 to 20 LT.....43

Figure 14. (a) Diurnal variations of atmospheric boundary layer averaged MA_PAN concentration in the NOURB-ALL, NOURB-OUT, NOURB-IN, and NOURB-NONE simulations in the urban area. (b) Diurnal variations of atmospheric boundary layer averaged MA_PAN concentration differences between NOURB-ALL simulation and NOURB-OUT, NOURB-IN, or NOURB-NONE simulation in the urban area. (c) Diurnal variations of atmospheric boundary layer averaged MA_PAN concentration differences between the NOURB-type and URB-type simulations in the urban area.....46

Figure 15. Diurnal variations of atmospheric boundary layer averaged contributions of individual processes to the MA_PAN concentration in the (a) NOURB-ALL, (b) NOURB-NONE, (c) NOURB-OUT, and (d) NOURB-IN simulations in the urban area from 06 to 20 LT.....47

List of Tables

Table 1. Simulation scenarios with different settings of land-use category, biogenic isoprene emission in the Seoul region, and biogenic isoprene emission in the surrounding region are considered.....	8
---	---

1. Introduction

The urban area is characterized by vast anthropogenic features. Because of anthropogenic features in the urban area, the skin temperature of the urban area is higher than the skin temperature of the rural area (e.g. Kim, 1992). This temperature increment and the changed land-use in the urbanized area provide local influences on airflow within the atmospheric boundary layer. When the skin temperature of the urban area is high enough and the synoptic wind is weak, the thermal forcing is dominant for the urban airflow (Wong and Dirks, 1978), wind blowing from surrounding areas to urban areas. This urban breeze circulation can be coupled with other local circulations such as mountain-valley breeze and/or sea breeze circulation (Ryu and Baik, 2013). Ryu et al. (2013) investigated the impacts of urban land-surface forcing on air quality in the Seoul Metropolitan area (SMA) using a high resolution meteorological model and a regional chemical transport model. They showed that the urban land-surface forcing strongly influences ozone concentration in the SMA under the weak synoptic condition.

Ozone is one of the most important pollutants in urban areas. Long-term ozone exposure reduces the lung function and increases the risk of

asthma admissions among children and nonsmoking adults (McDonnell et al., 1999; WHO, 2003; Lin et al., 2008). Also ozone damages roadside trees, rubbers, and textiles (Lee et al., 1996; Trahan and Peterson, 2007). Ozone is generated by photochemical reactions between NO_x ($= \text{NO} + \text{NO}_2$) and VOCs (Volatile Organic Compounds) in urban areas (Haagen-Smith and Fox, 1954). Unlike the rural area, the ozone concentration in urban areas depends on VOCs concentration rather than NO_x concentration (Milford et al., 1989, 1994; Sillman, 1999).

VOCs can be divided into two different groups by their origin; one is anthropogenic VOCs and the other is biogenic VOCs. VOCs effect on ozone concentration varies depending on the structure of individual species. Biogenic VOCs play an important role in producing ozone (Pierce et al., 1998). The effect of biogenic VOCs on ozone concentration is mainly observed in rural areas (Trainer et al., 1987). In addition, biogenic VOCs also affect ozone concentration in urban areas (Vogel et al., 1995; Bao et al., 2010).

Isoprene accounts for the most of biogenic VOCs, which is highly reactive species. The effect of isoprene on ozone concentration is quite large, not only in a rural area but also in an urban area (Trainer et al., 1987; Hellen et al., 2012). The maximum 1-hour averaged ozone

concentration in the urban area was perturbed by 10% due to the isoprene effect in Atlanta (Chameides et al., 1988). Li et al. (2007) showed that the 50% change in isoprene emission causes 5–25 ppb change in ozone concentration over the urban area, Houston.

In this study, the impacts of biogenic isoprene emission on ozone concentration in the SMA are investigated. SMA is the biggest metropolitan area in Korea, which consists of Seoul, Incheon, and part of Gyeonggi province, with a population of about 22 million. The topography of SMA is composed by several high mountains in the east side and coastal area in the west side. Seoul is in the basin which is located in the middle of SMA. That basin is surrounded by several mountains to the north, east, and south. Because of the geographical features of the urban area in the SMA, local circulations such as urban breeze, sea breeze, and valley breeze circulation can be developed in the daytime and interact with each other in the SMA under the weak synoptic wind condition (Ryu and Baik, 2013).

Because of its high reactivity, the lifetime of isoprene is very short (around 30 min) (Carslaw et al., 2000). It means that isoprene which is emitted from forests around the urban area cannot penetrate into the urban area. Therefore, the isoprene concentration in Seoul is relatively low (0.34 ppb in annual average) (Nguyen et al., 2009) and isoprene cannot directly

affect ozone concentration in the urban area. This feature gives us some question about which species link the biogenic isoprene emission and ozone concentration in the urban area.

To elucidate the impacts of biogenic isoprene emission and the effect of interaction between biogenic isoprene emission and urban breeze circulation on ozone concentration, simulations that the biogenic isoprene emission is fully or partly removed and/or the urban and industrial surfaces are replaced with the non-urban surface (cropland) are performed and their results are compared with the result from the control simulation.

2. Methodology

2.1 Meteorological modeling system

The Weather Research and Forecasting (WRF) model version 3.2 (Skamarock et al., 2008) is used to produce meteorological fields. For a better representation of urban surface characteristics, Seoul National University Urban Canopy Model (SNUUCM) (Ryu et al., 2011) is coupled

with the WRF model. Four domains with horizontal grid sizes of 27, 9, 3, and 1 km are considered. 43 vertical layers exist below the model top, and 16 vertical layers exist below 2 km height. The size of lowest vertical grid is around 35 m. The model is integrated for 96 hours from 00 UTC 22 June 2010 to 00 UTC 26 June 2010. The National Centers for Environmental Prediction (NCEP) final analysis data are used for the initial and boundary conditions. Other experimental setups are the same as those in Ryu and Baik (2013). To examine the effect of interaction between biogenic isoprene emission and urban breeze circulation on ozone concentration, additional simulations in which the urban and industrial land-use/land-cover categories in the innermost domain (Fig. 1b) are replaced with the cropland land-use/land-cover category are performed following Ryu et al. (2013).

2.2 Air quality modeling system

The Community Multiscale Air Quality (CMAQ) modeling system version 4.7.1 is used in this study. The results of WRF model simulations are used as the meteorological inputs. In the air quality simulations, three domains with horizontal grid sizes of 9, 3, and 1 km are considered (Fig.

1a). The default profiles in the CMAQ model are used for the initial and boundary conditions for the outermost domain. The 29 vertical layers are used in this study. The lower 22 layers are the same as the layers used in the WRF simulations. The model is integrated for 96 hours, and the simulation results from 15 UTC 23 June to 15 UTC 24 June (00 – 24 LT June 24) are analyzed. The Statewide Air Pollution Research Center version 99 (SAPRC-99) chemical mechanism (Carter, 2000), which includes 77 chemical species and 224 chemical reactions, and the fifth-generation model CMAQ aerosol module (Foley et al., 2010) are used in this study. The Yamartino scheme (Yamartino, 1993) and the Asymmetric Convective Model version 2 (ACM2) vertical diffusion scheme (Pleim, 2007) are adopted.

The hourly anthropogenic emission data for all domains are estimated from 2007 Clean Air Policy Support System of South Korea (CAPSS) using the Sparse Matrix Operator Kernel Emissions (SMOKE) system (Houyoux et al., 2000). The Model of Emissions of Gases and Aerosols from Nature (MEGAN) (Guenther et al., 2006) is used to estimate hourly biogenic emission data. The biogenic isoprene emission depends on the land-use/land-cover categories (Fig. 1b). In the SMA, the biogenic isoprene emission rate in the forest is higher than that in the urban area (Fig. 1c).

2.3 Simulation scenarios

All of the simulation scenarios are summarized in Table 1. ALL simulation is a control simulation which consists of real land-use/land-cover categories and real biogenic isoprene emission (Fig. 1c). OUT simulation is the same as the ALL simulation except that the biogenic isoprene emission in the Seoul region is completely removed (Fig. 1e). IN simulation is the same as the ALL simulation except that the biogenic isoprene emission in the surrounding regions is completely removed (Fig. 1f). NONE simulation is a simulation which consists of real land-use/land-cover categories, but no biogenic isoprene emission exists (Fig. 1d). NOURB-ALL simulation is a simulation with replaced land-use/land-cover category. NOURB-OUT, NOURB-IN, and NOURB-NONE simulations are the same as the OUT, IN, and NONE simulations except for the land-use/land cover category. Both anthropogenic and biogenic emissions in the every simulation except for biogenic isoprene emission are set to be identical to each other. ALL, OUT, IN, and NONE simulations are grouped as URB-type simulations and NOURB-ALL, NOURB-OUT, NOURB-IN, and NOURB-NONE simulations are grouped as NOURB-type simulations.

Table 1. Simulation scenarios with different settings of land-use category, biogenic isoprene emission in the Seoul region, and biogenic isoprene emission in the surrounding region are considered.

Simulation	Land-use category	Biogenic isoprene emission	
		In the Seoul region	In the surrounding region
ALL	urban+industrial	Yes	Yes
OUT	urban+industrial	No	Yes
IN	urban+industrial	Yes	No
NONE	urban+industrial	No	No
NOURB-ALL	cropland	Yes	Yes
NOURB-OUT	cropland	No	Yes
NOURB-IN	cropland	Yes	No
NOURB-NONE	cropland	No	No

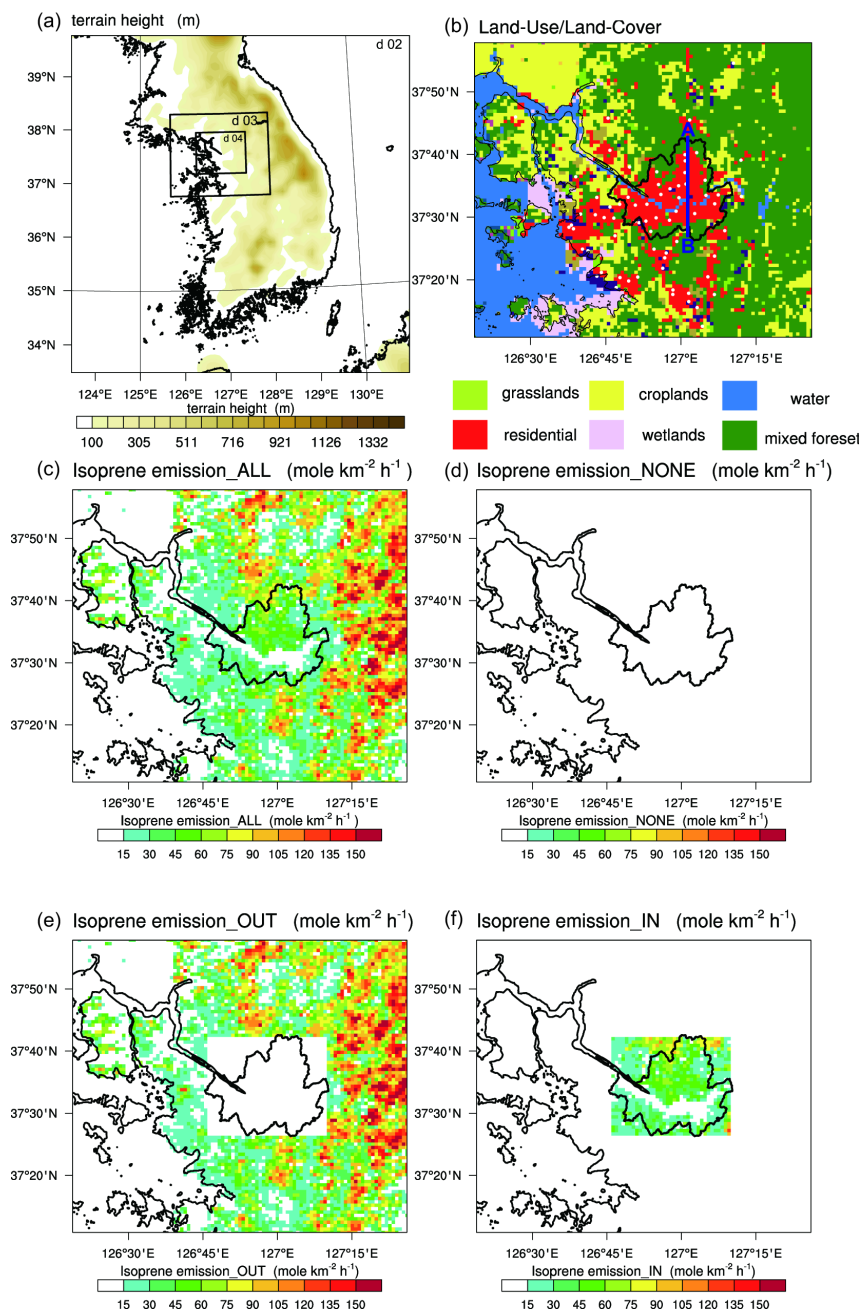


Figure 1. (a) CMAQ simulation domains with terrain height and (b) land-use/land-cover in the innermost domain. The white circles

indicate air quality monitoring sites, and the blue line indicates the location of vertical cross section that is shown in Figs. 10 and 11. The isoprene emission rate in the (c) ALL, (d) NONE, (e) OUT, and (f) IN simulations at 15 LT 24 June 2010 in the innermost domain.

3. Results and discussion

3.1 Model validation

The ozone concentration in the ALL simulation is used to validate the air quality model (Fig. 2). The diurnal variations of observed ozone concentration at air quality monitoring sites (marked by white circles in Fig. 1b) and simulated ozone concentration at the same locations in the innermost domain are compared in Fig. 2a. The model reproduces the maximum and minimum of ozone concentration quite well. Although the model underestimates ozone concentration in the late afternoon, the model result captures the diurnal variation of ozone concentration on average. Figure 2b shows a scatter plot of the simulated ozone concentrations and the observed ozone concentrations with performance statistics. Although ozone concentrations in the ALL simulation are slightly underestimated in the afternoon, these are well correlated with the observed ozone concentrations. The mean normalized bias error (MNBE) and the mean normalized gross error (MNGE) with observed ozone concentrations above a 40 ppb threshold

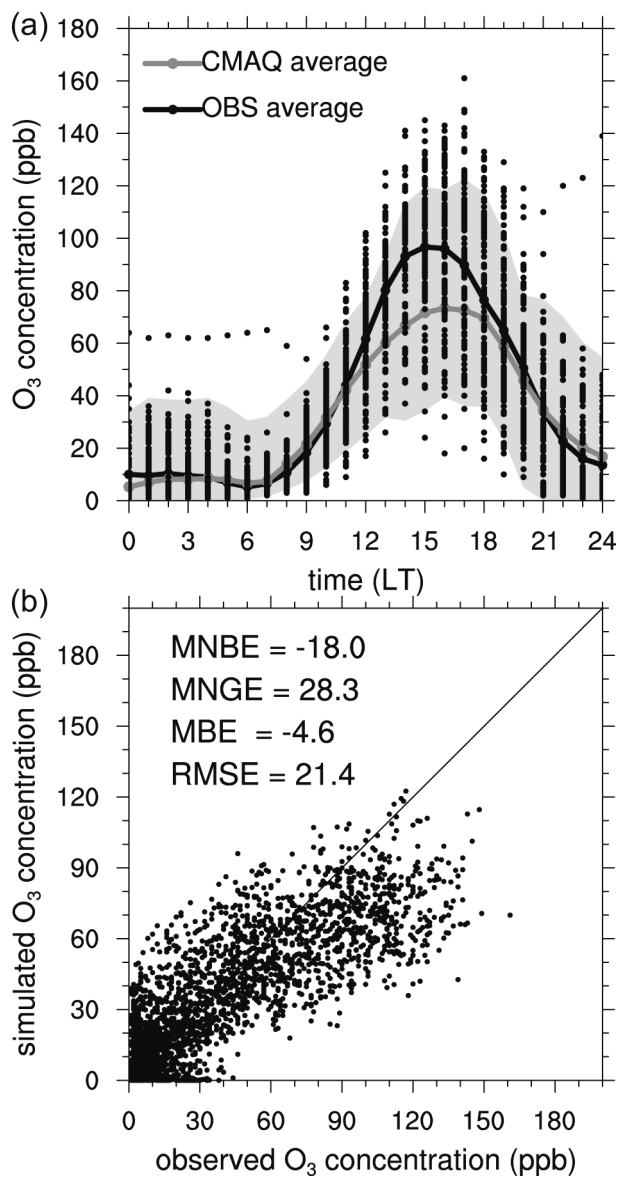


Figure 2. (a) Diurnal variations of observed and simulated ozone concentration near the surface on 24 June 2010. The dots and shading indicate the observed ozone concentration at air quality monitoring sites and

the simulated ozone concentration at the corresponding grids, respectively. The black and grey lines indicate the average ozone concentration of observation and simulation, respectively. (b) Scatter plot of observed ozone concentration versus simulated ozone concentration on 24 June 2010. The unit of MNBE and MNGE is %, and the unit of MBE and RMSE is ppb.

are calculated. The MNBE and MNGE are -18% and 28%, respectively. The performance criteria which are recommended by the US Environmental Protection Agency (USEPA) are that the MNBE is within $\pm 15\%$ and the MNGE is less than or equal to 35% (USEPA, 1991). The simulation results also satisfy the criterion for the MNGE, but simulation results slightly exceed the criterion for the MNBE. The mean bias error is -4.6 ppb, and the root-mean-square-error (RMSE) is 21.4 ppb. This slight exceedance of the MNBE is attributed to the underestimation of the ozone concentrations in the afternoon.

3.2 Impacts of biogenic isoprene emission

To understand the impacts of biogenic isoprene emission on ozone concentration in the SMA, the results in the ALL, OUT, IN, and NONE simulations are compared. Figure 3 shows the diurnal variations of atmospheric boundary layer averaged concentrations of ozone and isoprene (Fig. 3a and c, respectively) in the ALL, OUT, IN, and NONE simulations and the ozone concentration differences between the ALL simulation and the OUT, IN, or NONE simulation (Fig. 3b) in the urban area. The daily

maximum ozone concentrations in the ALL, OUT, IN, and NONE simulations are 82, 78, 52, and 45 ppb, respectively. The ozone concentration in the ALL simulation is always higher than that in the OUT simulation, and the ozone concentration in the OUT simulation is always higher than that in the IN simulation. Unlike in the ALL and OUT simulations, the ozone concentrations in the IN and NONE simulations are not largely perturbed (less than 1 ppb) in the afternoon (from 15 to 17 LT). The daily maxima of ozone concentration appear at 18 LT in the ALL and OUT simulations. However, the daily maxima of ozone concentration in the IN and NONE simulations appear much earlier than in the ALL and OUT simulations, which are at 15 and 16 LT, respectively. The daily maxima of ozone concentration difference appear at 16 LT (ALL - OUT) and 18 LT (ALL - IN and ALL - NONE), when the urban breeze circulation is well developed. On average, the daytime (from 06 to 19 LT) ozone concentration in the ALL simulation is 3.2, 14.4, and 17.1 ppb higher than daytime ozone concentration in the OUT, IN, and NONE simulations, respectively. In the nighttime (from 00 to 05 LT and from 20 to 24 LT), ozone concentration in the ALL simulation is 0.3, 9.2, and 9.5 ppb higher than ozone concentration in the OUT, IN, and NONE simulations, respectively. The biogenic isoprene emission rate depends on air temperature and light

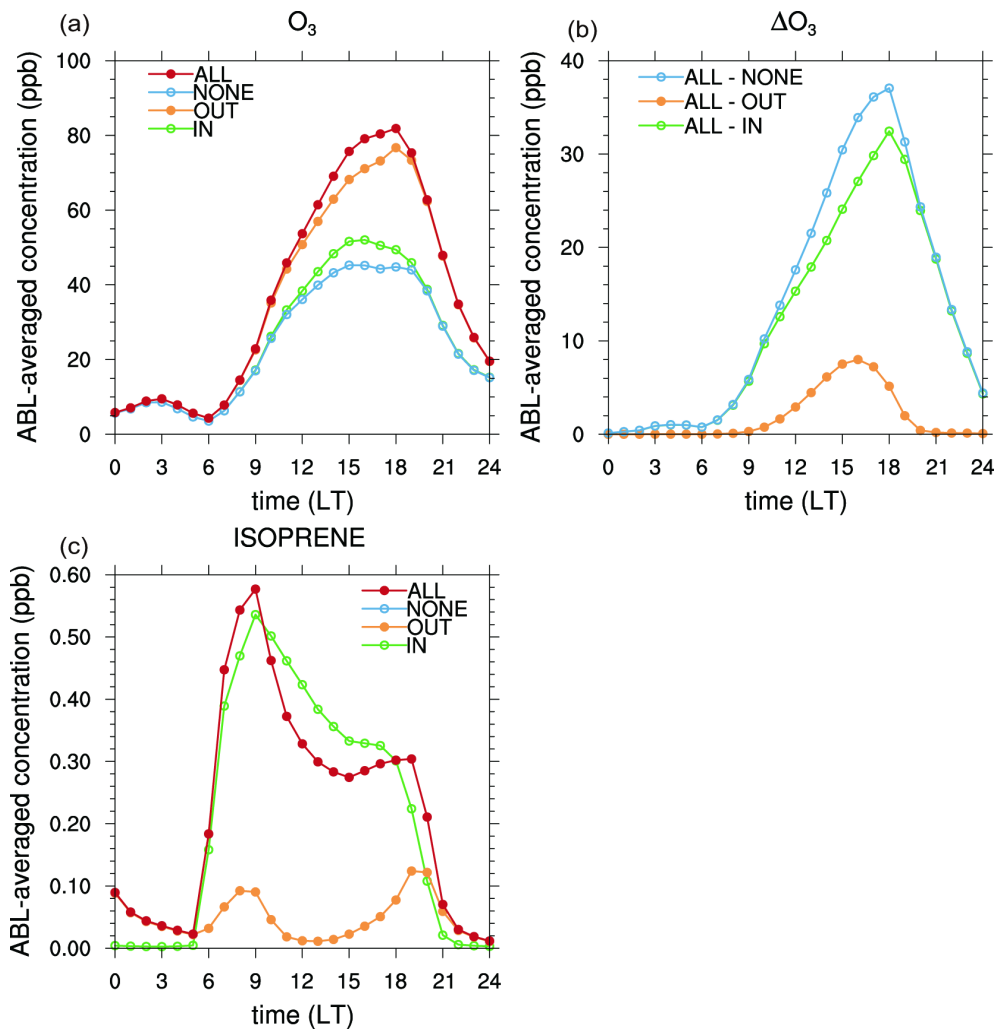


Figure 3. Diurnal variations of atmospheric boundary layer averaged concentrations of (a) ozone and (c) isoprene in the ALL, OUT, IN, and NONE simulations in the urban area. (b) Diurnal variations of ozone concentration differences between the ALL simulation and the OUT, IN, or NONE simulation in the urban area.

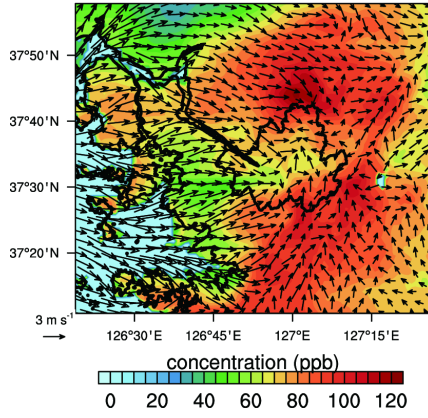
intensity (Guenther et al., 1993, 1995; Bao et al., 2008). Because of no solar radiation in the nighttime, the biogenic isoprene emission in the nighttime is almost zero. Hence, the impacts of biogenic isoprene emission on the ozone concentration are smaller in the nighttime than in the daytime. The ozone concentration difference between the ALL and IN simulations is relatively larger than the difference between the ALL and OUT simulations. This implies that the biogenic isoprene emission in the surrounding area of Seoul is more important to the ozone concentration in Seoul rather than the biogenic isoprene emission in Seoul.

The diurnal variations of isoprene concentration are quite different from the diurnal variations of ozone concentration. In the ALL and IN simulations, the isoprene concentrations rapidly increase after sunrise and reach the daily maximum in the morning (09 LT). In the daytime, the isoprene concentrations in the ALL and IN simulations slowly decrease until evening. In the OUT simulation, the isoprene concentration slowly increases after sunrise and reaches the local maximum in the morning. In the forenoon, the isoprene concentration in the OUT simulation slowly decreases and reaches local minimum at noon. In the afternoon, the isoprene concentration in the OUT simulation slowly increases. In the evening, the isoprene concentration is slightly (in the IN simulation) or considerably (in

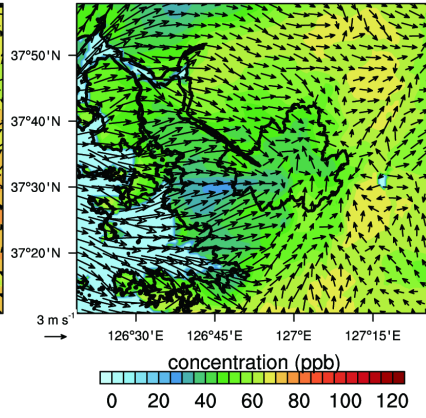
the ALL and OUT simulations) increased. The increments in the morning are due to the biogenic isoprene emission. However, the increments in the evening are due to the entrainment of isoprene that is emitted from the surrounding area of Seoul and the lack of OH radical which converts isoprene to smaller molecules after sunset. Unlike the ozone concentration, the isoprene concentration in the IN simulation is higher than that in the OUT simulation until 19 LT. This result also implies that isoprene is confined in the area where it is emitted from.

Figure 4 shows the atmospheric boundary layer averaged ozone concentration and horizontal wind fields at the lowest model level at 15 LT in the four simulations (ALL, OUT, IN, and NONE) and the ratio of ozone concentration difference between the ALL simulation and the OUT or IN simulation to ozone concentration in the ALL simulation. As shown in Fig. 3, the ozone concentration in the urban area is generally higher when the biogenic isoprene emission in the surrounding area exists (ALL and OUT simulations) than when the biogenic isoprene emission in the surrounding area does not exist (IN and NONE simulations). The ozone concentration in the surrounding area is generally higher than that in the urban area, even in the simulation in which the biogenic isoprene emission is completely removed. The wind near the surface converges toward the urban area in the

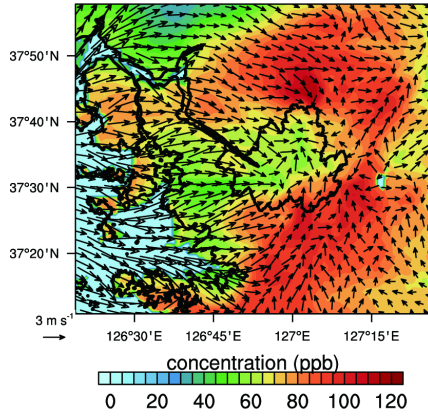
(a) O₃ at 15 LT (ALL)



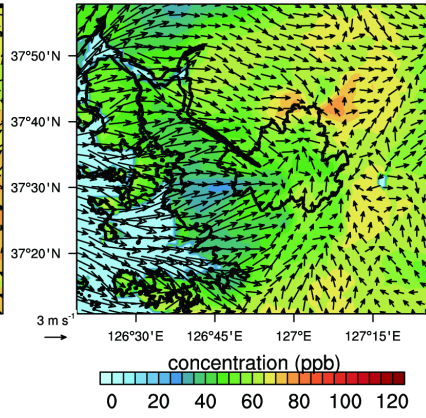
(b) O₃ at 15 LT (NONE)



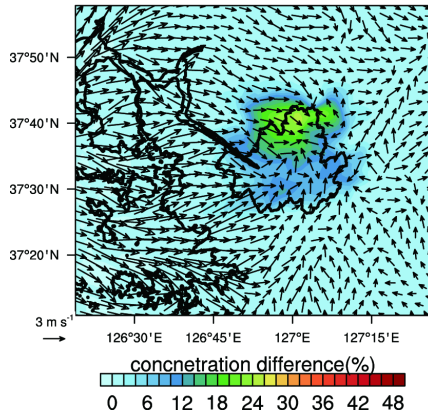
(c) O₃ at 15 LT (OUT)



(d) O₃ at 15 LT (IN)



(e) ΔO₃ at 15 LT (ALL-OUT)



(f) ΔO₃ at 15 LT (ALL-IN)

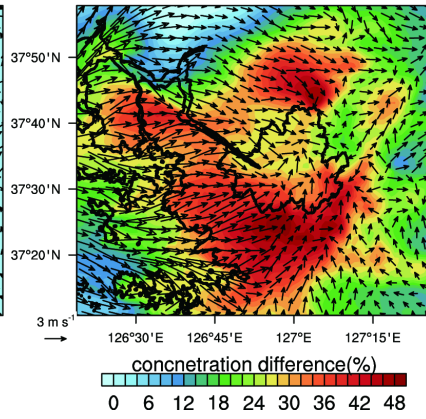


Figure 4. Horizontal distributions of atmospheric boundary layer averaged ozone concentrations in the (a) ALL, (b) NONE, (c) OUT, and (d) IN simulations, and the ratio of the ozone concentration differences between the ALL simulation and the (e) OUT or (f) IN simulation to the ozone concentration in the ALL simulation at 15 LT. Horizontal wind fields are at the lowest model level.

northern and southeastern parts of Seoul. In Fig. 4e, the ratio over the mountains is larger than that in the urban area where urban breeze converges. Moreover, the ratio over the urban breeze convergence zone is higher than that in the other urban areas in Seoul in Fig. 4f. These results also indicate that the urban breeze circulation is important to the impacts of the biogenic isoprene emission on the ozone concentration in the urban area.

To evaluate the contributions of individual processes to the changes in ozone concentration, an integrated process rate (IPR) analysis which is implemented in the CMAQ is performed. Figure 5 shows the atmospheric boundary layer averaged contributions of individual processes to the ozone concentration in the urban area from 06 to 20 LT. Not only in the ALL and IN simulations but also in the OUT simulation, the chemical reactions are the largest ozone source in the urban area in the afternoon. The ozone transport rate (sum of advection and diffusion rates) is relatively smaller than the ozone production rate in the afternoon in the ALL, OUT, and IN simulations. In the NONE simulation, unlike other simulations, the ozone production rate is smaller than the ozone transport rate (Fig. 5b). However, in the nighttime, ozone is decomposed by chemical reactions and is transported from the surrounding area into the urban area. On average, the ozone production rates are 5.9, 3.8, 2.6, and 0.8 ppb h⁻¹ from 11 to 15 LT

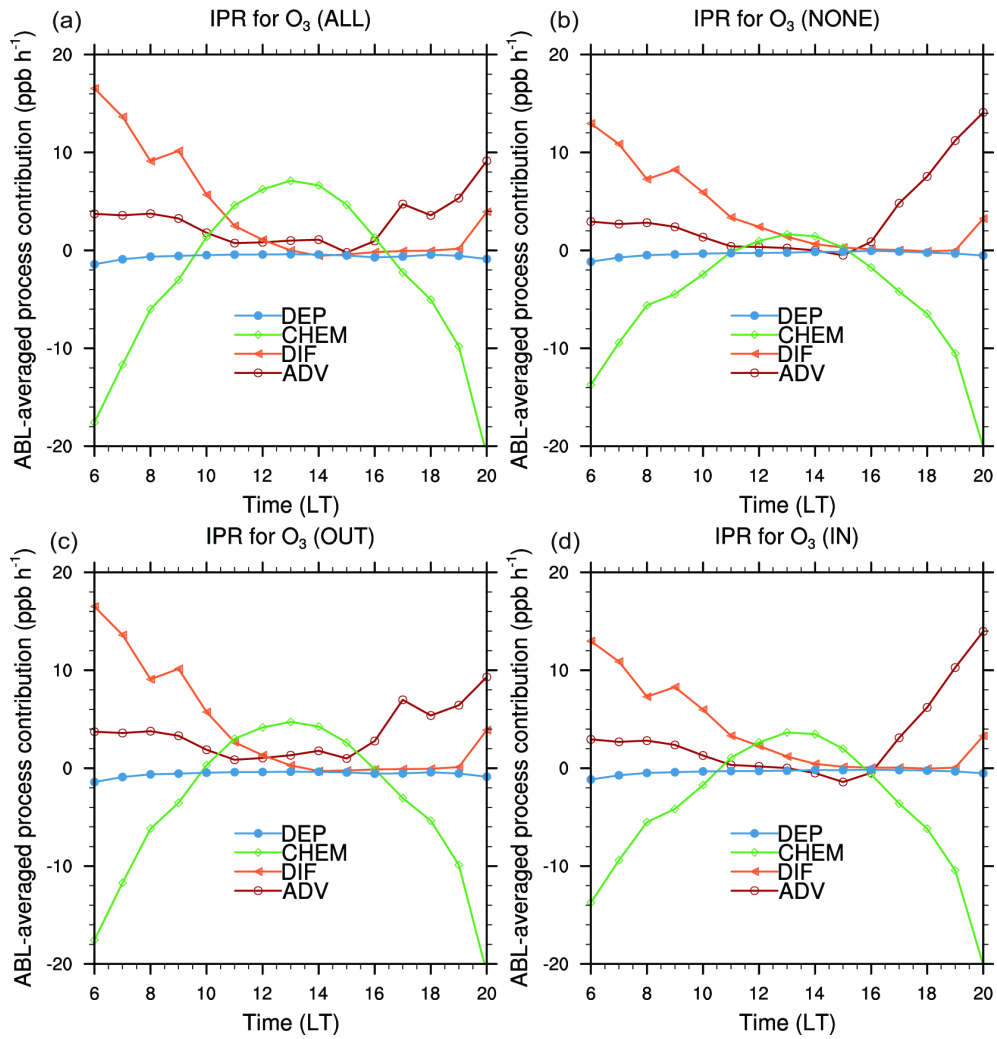


Figure 5. Diurnal variations of atmospheric boundary layer averaged contributions of individual processes to the ozone concentration from 06 to 20 LT in (a) ALL, (b) NONE, (c) OUT, and (d) IN simulations in the urban area.

in the ALL, OUT, IN, and NONE simulations, respectively. Moreover, the ozone transport rates are 1.2, 1.9, 1.2, and 1.7 ppb h⁻¹ from 11 to 15 LT in the ALL, OUT, IN, and NONE simulations, respectively. In the daytime, NO_x and VOCs are continuously emitted from both anthropogenic and biogenic sources. The emitted VOCs are oxidized by OH radical and produce HO₂ and RO₂ radicals. These HO₂ and RO₂ radicals convert NO to NO₂. In the daytime, NO₂ is dissociated into the NO and O^{3p}, and the O^{3p} reacts with O₂ and finally produces ozone. In the nighttime, NO is continuously emitted from anthropogenic sources and reacts with ozone. Because there is no sunlight in nighttime, NO₂ photolysis which is the most important reaction to produce ozone in the troposphere cannot occur. As a result, ozone is converted to O₂ by chemical reactions and compensated by advection and diffusion in the nighttime.

The 5-hour averaged vertical profiles of ozone concentration in the urban area for the period from 11 to 15 LT in different simulations are quite similar to each other except for the magnitude of the ozone concentration (not shown). Figure 6 shows the 5-hour averaged vertical profiles of contributions of individual processes to the ozone concentration in the urban area for the period from 11 to 15 LT. Ozone is produced in the upper parts of the atmospheric boundary layer (layer number ≥ 3 in

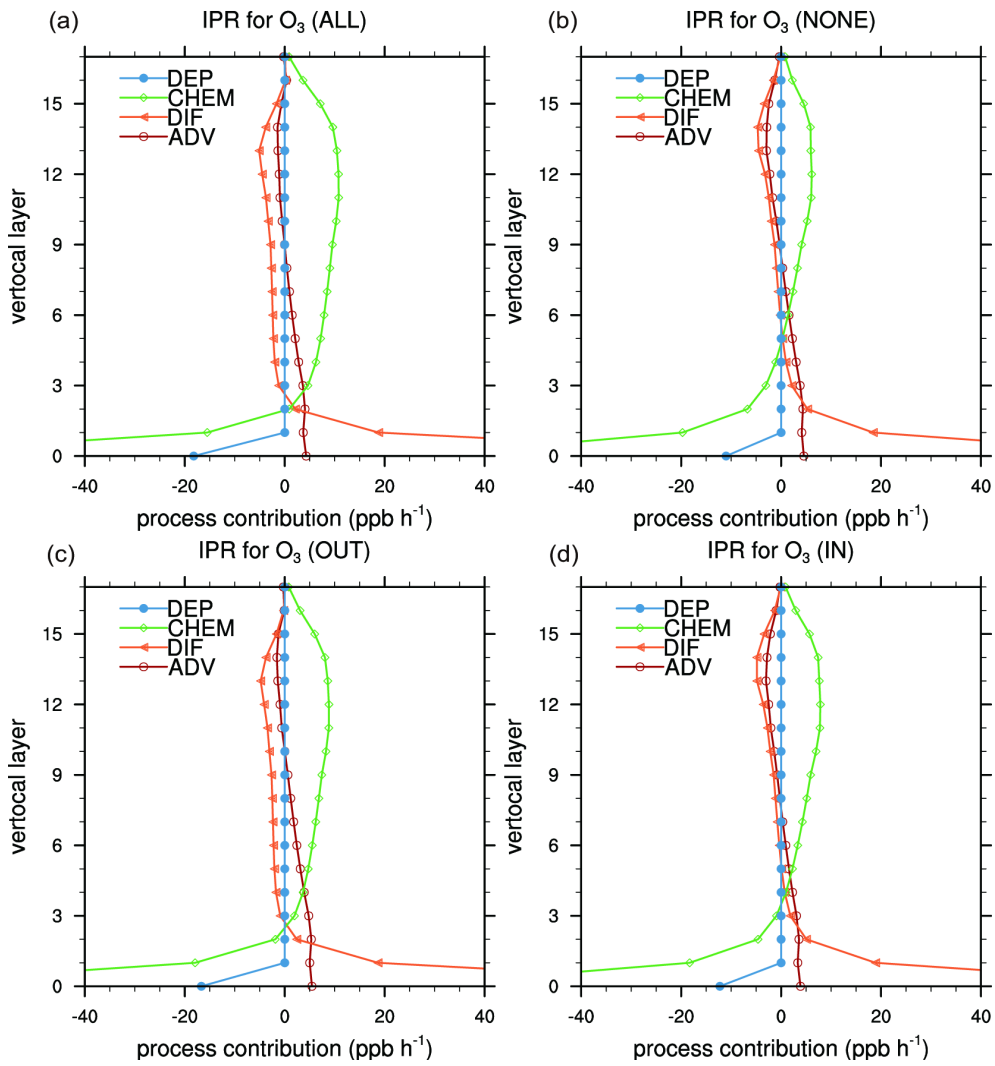


Figure 6. 5-hour averaged vertical profiles of contributions of individual processes to the ozone concentration averaged over the urban area for the period from 11 to 15 LT in the (a) ALL, (b) NONE, (c) OUT, and (d) IN simulations.

the ALL and OUT simulations, ≥ 4 in the IN and NONE simulations) and is consumed in the lower parts because of NO-titration reaction. Ozone diffused from the upper parts to the lower parts compensates the ozone consumption in the lower parts of the atmospheric boundary layer.

The results presented above also indicate that some species (hereafter, key species) which are related to isoprene chemistry are transported from the surrounding area into the urban area in the afternoon when the urban breeze prevails. These transport of key species link the biogenic isoprene emission and the ozone concentration in the urban area.

Key species have some strict constraints and some lenient constraints. First, they must be transported from the surrounding area into the urban area in the afternoon when the urban breeze prevails in the OUT simulation, and this transport does not occur in the IN and NONE simulations. Second, they must be converted into another species in the urban area in the OUT simulation, and they must be produced in the urban area in the IN simulation. Third, their chemical lifetimes should not be too long (e.g., HNO_3) and too short (e.g., radicals). At last, their concentration differences between the ALL and OUT simulations should be smaller than those between the ALL and IN simulations.

To find the key species, IPR analysis for species which are involved

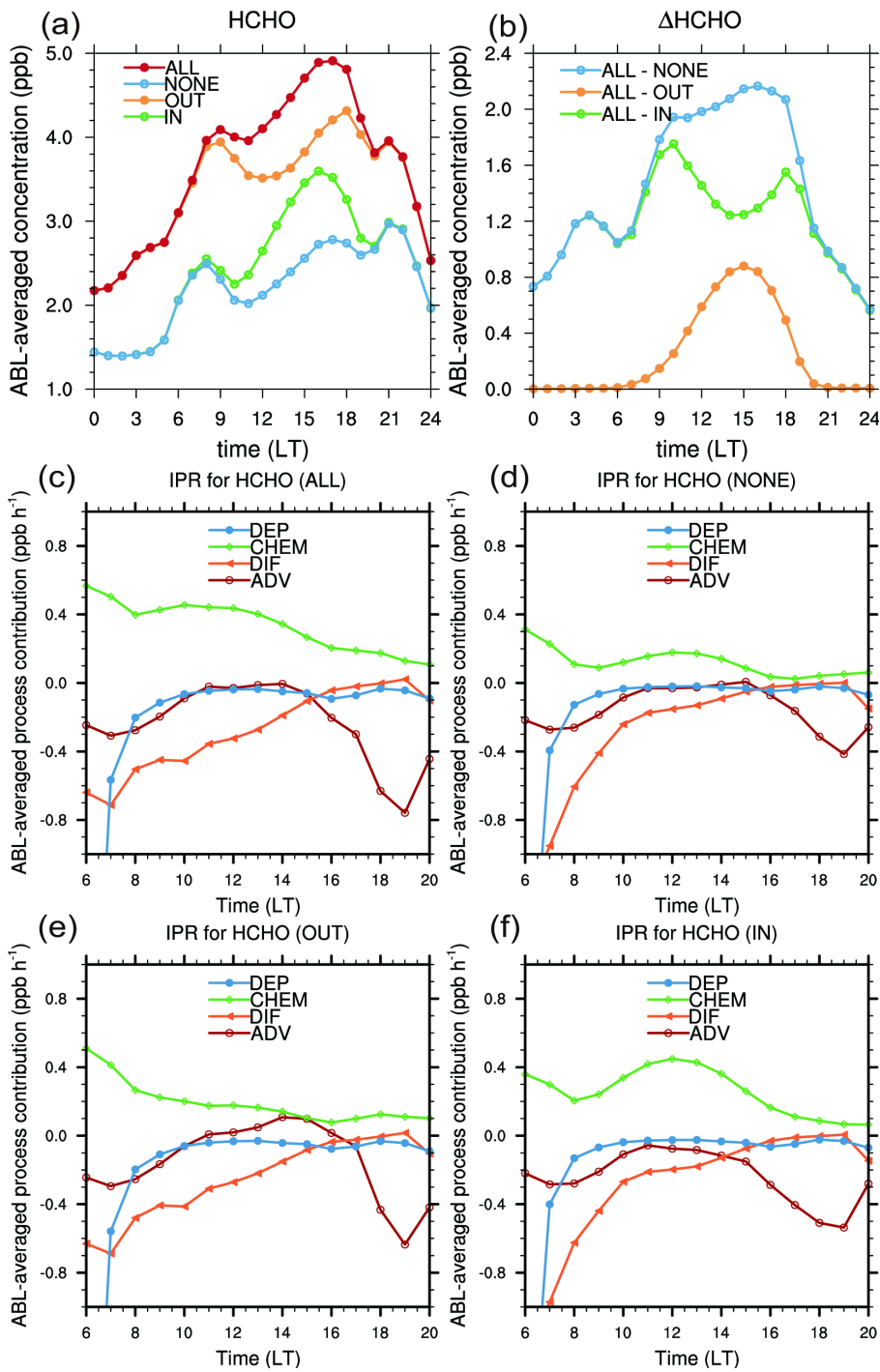


Figure 7. (a) Diurnal variations of atmospheric boundary layer averaged HCHO concentration in the ALL, OUT, IN, and NONE simulations. (b) Diurnal variations of HCHO concentration difference between the ALL simulation and OUT, IN, or NONE simulation in the urban area. Diurnal variations of atmospheric boundary layer averaged contributions of individual processes to the HCHO concentration from 06 to 20 LT in the (c) ALL, (d) NONE, (e) OUT, and (f) IN simulations in the urban area .

in isoprene chemistry is performed, and the concentrations of the species in the ALL, OUT, IN, and NONE simulations are compared. Several species such as formaldehyde (HCHO), acetaldehyde (CH₃CHO), and formic acid (HCOOH) are known as key species for isoprene chemistry (Geng et al., 2011). HCHO satisfies constraints on the concentration difference (Fig. 7a and b) and chemical lifetime. However, HCHO is not transported from the surrounding area into the urban area and is produced in the urban area (Fig. 7c, d, e, and f). Not only HCHO but also other species in isoprene chemistry except MA_PAN do not satisfy the constraints. Methyl vinyl ketone does not satisfy the constraints on the concentration difference. CH₃CHO and HCOOH do not satisfy the constraints on transport.

Figure 8 shows the diurnal variations of atmospheric boundary layer averaged concentrations of MA_PAN (Fig. 8a), MA_PAN concentration differences between the ALL simulation and OUT, IN, or NONE simulation (Fig. 8b), and contributions of individual processes to the MA_PAN concentration from 06 to 20 LT in the ALL, NONE, OUT, and IN simulations (Fig. 8c, d, e, and f, respectively) in the urban area. MA_PAN is a lumped chemical group which is implemented in the SAPRC-99 chemical mechanism. MA_PAN contains methacryloyl peroxy nitrate (MPAN) and other peroxyacyl nitrates (PANS) from acroleins. Some

previous studies have indicated that MPAN that is lumped in MA_PAN can be an indicator of the air mass from the rural area affects the urban area (Williams et al., 1997). In the SAPRC-99 chemical mechanism, MA_PAN is produced by a reaction between NO_2 and MA_RCO₃, a group of peroxyacyl radicals produced from methacrolein and other acroleins, and is thermally decomposed into NO_2 and MA_RCO₃. The MA_PAN concentration in the OUT simulation is generally higher than the MA_PAN concentration in the IN simulation (Fig. 8a), and the MA_PAN concentration difference between the ALL and OUT simulation is lower than the MA_PAN concentration difference between the ALL and IN simulation (Fig. 8b). In the OUT simulation, MA_PAN is advected from the surrounding area into the urban area and is decomposed into MA_RCO₃ and NO_2 (Fig. 8e). The maxima of MA_PAN advection rate appear at 17 LT when the urban breeze circulation is well developed and the sea breeze penetrates into the urban area in the ALL and OUT simulations (Fig. 8c and e). In the IN simulation, MA_PAN is produced in the urban area and is transported from the urban area into the surrounding area (Fig. 8f). The daily maxima of MA_PAN concentration in the IN simulation appear at 15 LT when the daily maxima of ozone concentration is appeared in the IN simulation. The MA_PAN concentration in the NONE simulation is almost negligible compared to that in other

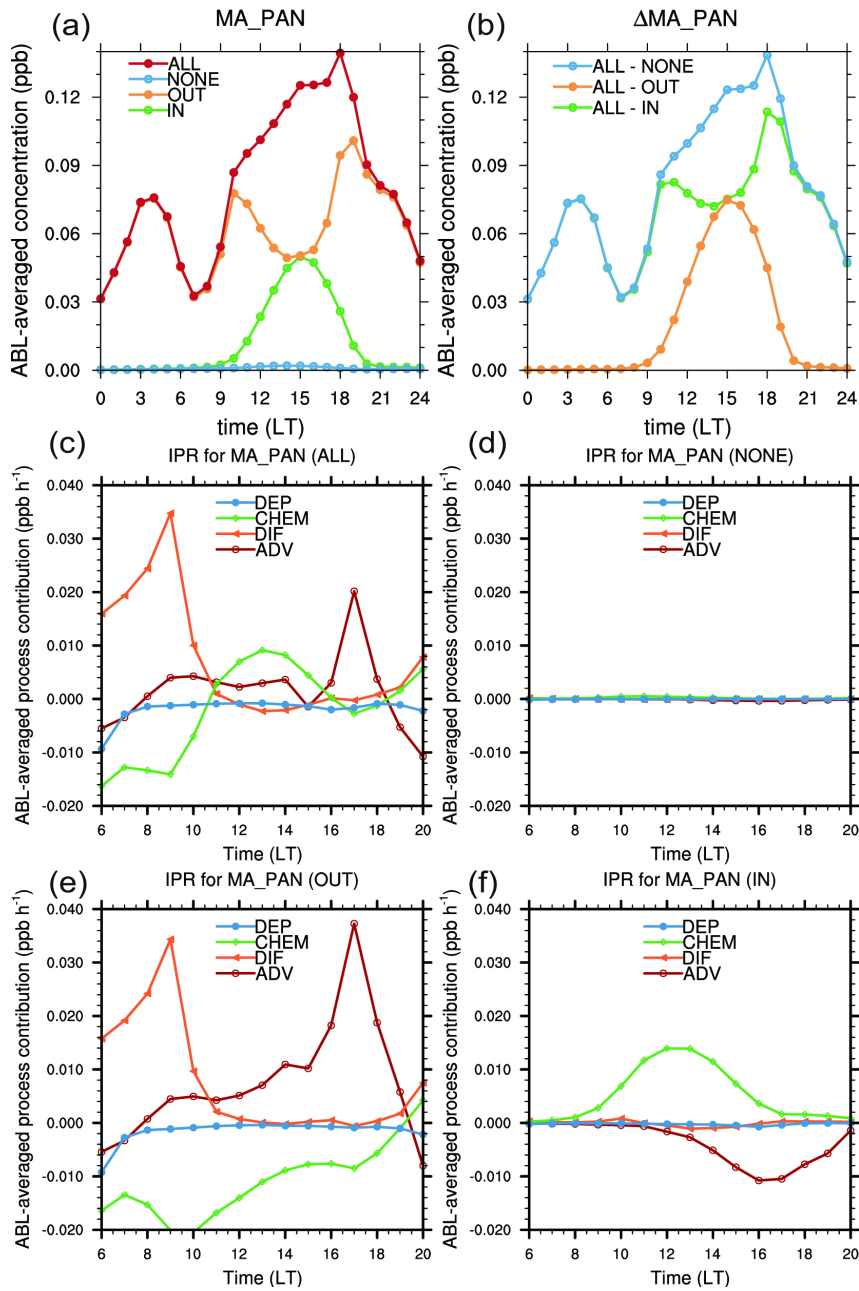


Figure 8. (a) Diurnal variations of atmospheric boundary layer averaged MA_PAN concentration in the ALL, OUT, IN, and NONE simulations in

the urban area. (b) Diurnal variations of atmospheric boundary layer averaged MA_PAN concentration differences between the ALL simulation and the OUT, IN, or NONE simulation in the urban area. Diurnal variations of atmospheric boundary layer averaged contributions of individual processes to the MA_PAN concentration from 06 to 20 LT in the (c) ALL, (d) NONE, (e) OUT, and (f) IN simulations in the urban area.

simulations (Fig. 8a). Also, contribution of individual processes on the MA_PAN concentration in the NONE simulation is less than one tenth of that in other simulations (Fig. 8d). In the ALL simulation, MA_PAN is produced in the urban area from 11 to 16 LT and is transported from the surrounding area into the urban area in the daytime (Fig. 8c).

Figure 9 shows the 5-hour averaged vertical profiles of MA_PAN concentrations and the contributions of individual processes to the MA_PAN concentration in the urban area for the period from 11 to 15 LT similar to Fig. 6. The maxima of MA_PAN concentration appear at the top of the atmospheric boundary layer in the three simulations except for the NONE simulation. However, the MA_PAN concentrations are almost constant in the atmospheric boundary layer (Fig. 9a). In the OUT simulation, MA_PAN is advected from the surrounding area into the urban area especially in the lower parts of the atmospheric boundary layer and is decomposed. Because of non-negligible concentration difference between upper and lower parts of the atmospheric boundary layer, which is caused by different chemical reaction rate, MA_PAN is diffused from the upper to the lower parts of the atmospheric boundary layer (Fig. 9d). In the IN simulation, MA_PAN is produced in the urban area and is advected from the urban area into the surrounding area in the atmospheric boundary layer. Although isoprene and

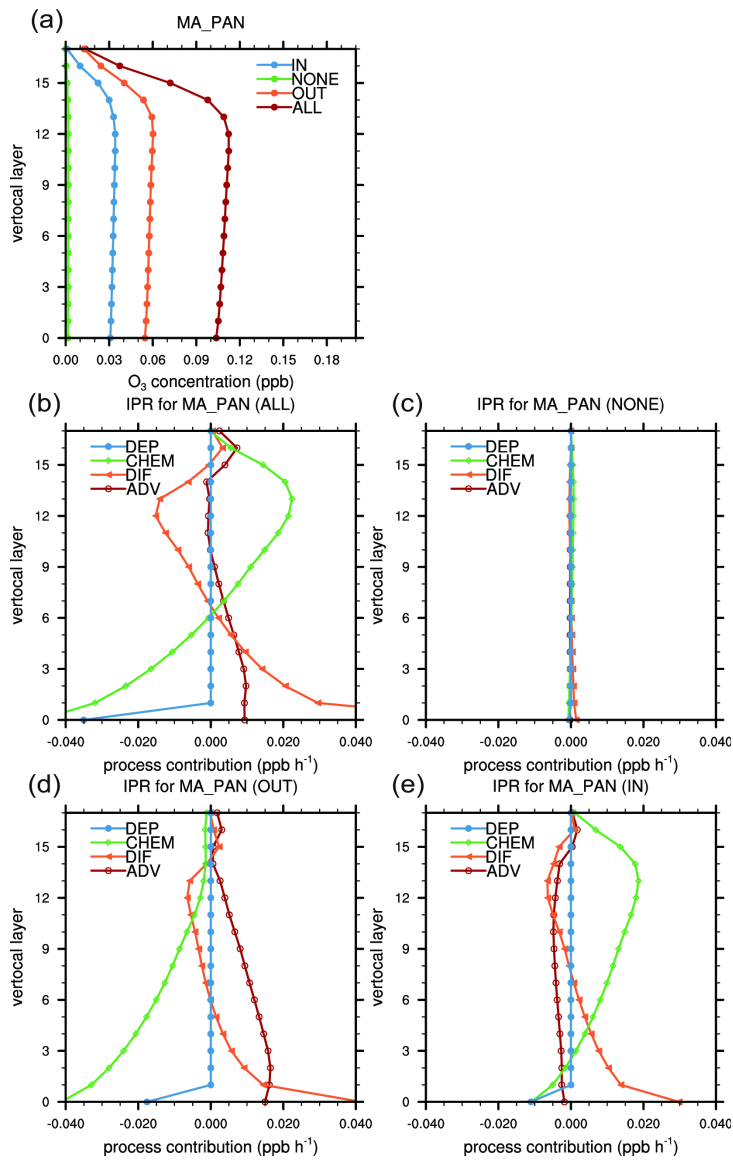


Figure 9. 5-hour averaged vertical profiles of (a) MA_PAN concentrations in the ALL, OUT, IN, and NONE simulations, and contributions of individual processes to the MA_PAN concentration in the (b) ALL, (c) NONE, (d) OUT, and (e) IN simulations in the urban area.

NO₂ are emitted from the surface, the maxima of MA_PAN production rate appear at the top of the atmospheric boundary layer (Fig. 9e). The contributions of individual processes to the MA_PAN concentration in the ALL simulation are the combination of those in the OUT and IN simulations. In the ALL simulation, MA_PAN is produced in the upper parts of the atmospheric boundary layer, similar to the IN simulation, and is advected from the surrounding area into the urban area in the lower parts of the atmospheric boundary layer, similar to the OUT simulation (Fig. 9b). As already seen in Fig. 8, MA_PAN concentration and the contributions of individual processes to the MA_PAN concentration in the NONE simulation are almost zero (Fig. 9a and c).

To find the relationship between MA_PAN and ozone in detail, the vertical cross sections of contributions of the transport and the chemical reactions to the MA_PAN concentration along the line A-B in Fig. 1b in the ALL, OUT, and IN simulations are shown in Fig. 10. Similar to Fig. 10, Fig. 11 shows the vertical cross sections of the ozone concentration and the contributions of chemical reactions to the ozone concentration. As already seen in Fig. 8, MA_PAN is transported from the surrounding area into the urban area following the urban breeze in the ALL and OUT simulations (Fig. 10a and c). Also, this transported MA_PAN is decomposed

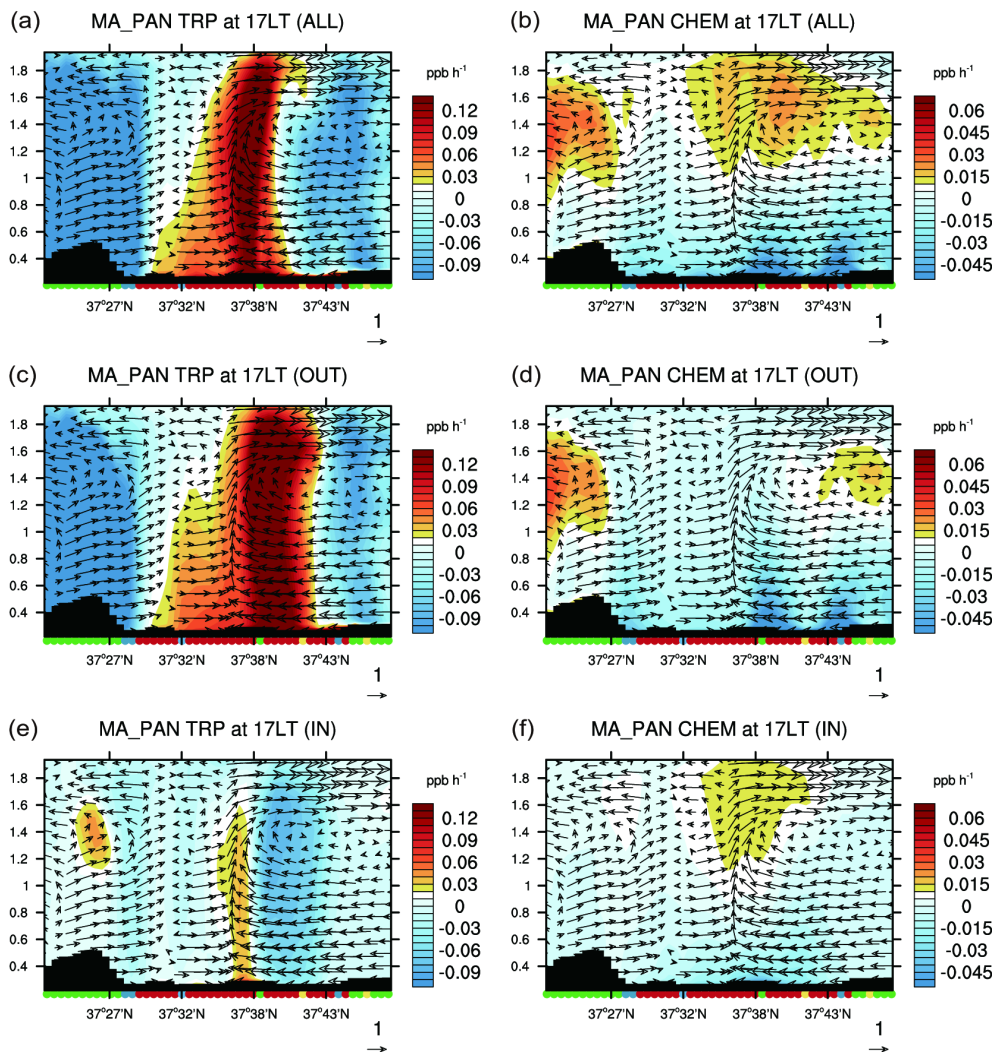


Figure 10. Vertical cross sections of contribution of transport to the MA_PAN concentration in the (a) ALL, (c) OUT, and (e) IN simulations. Vertical cross sections of contribution of chemical reaction to the MA_PAN concentration in the (b) ALL, (d) OUT, and (f) IN simulations at 17 LT.

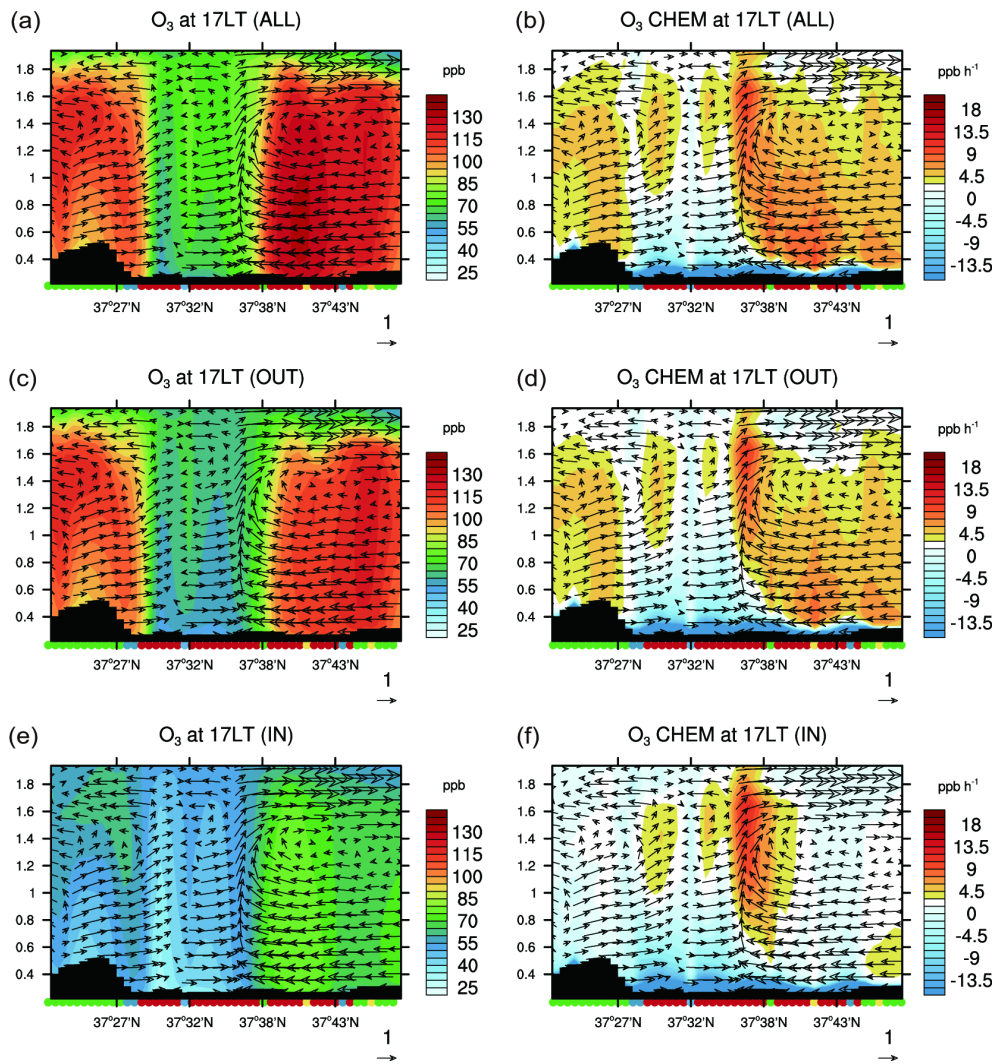


Figure 11. Vertical cross sections of ozone concentration in the (a) ALL, (c) OUT, and (e) IN simulations. Vertical cross sections of contribution of chemical reactions to the ozone concentration in the (b) ALL, (d) OUT, and (f) IN simulations at 17 LT.

into another species near the surface of the urban area similar to what we have seen above (Fig. 10b and d). In the IN simulation, MA_PAN is not transported from the surrounding area (Fig. 10e). MA_PAN is produced in the upper parts of atmospheric boundary layer and is transported just inside the urban area (Fig. 10e and f). The ozone concentration above the urban area where MA_PAN is transported is higher than that in other urban areas in the ALL and OUT simulations (Fig. 10a and c, and Fig. 11a and c). Ozone is produced above the urban area, especially where MA_PAN is transported and is decomposed into another species (Fig. 10b and d, and Fig. 11b and d). In the IN simulation, ozone is produced above the urban area where urban breeze converges. In that area, MA_PAN is also transported, but the magnitude of ozone production rate is much smaller than that in the ALL and OUT simulations (Fig. 10e and f, and Fig. 11e and f).

3.3 Effect of interaction between biogenic isoprene emission and urban breeze circulation

As mentioned in Ryu et al. (2013) and in Sect. 3.2, local circulations

such as urban breeze circulation are very important to the ozone concentration in the urban area. To evaluate the effect of interaction between biogenic isoprene emission and urban breeze circulation on the ozone concentration in the SMA, the results from the NOURB-ALL, NOURB-OUT, NOURB-IN, and NOURB-NONE simulations are compared to each other and compared with the results from the ALL, OUT, IN, and NONE simulations, respectively.

Figure 12 shows the diurnal variations of the atmospheric boundary layer averaged concentration of ozone and isoprene (Fig. 12a and c, respectively) in the NOURB-ALL, NOURB-OUT, NOURB-IN, and NOURB-NONE simulations, the ozone concentration differences between the NOURB-ALL simulation and NOURB-OUT, NOURB-IN, or NOURB-NONE simulation (Fig. 12b), and the ozone concentration differences between the URB-type simulations and NOURB-type simulations in the urban area. The daily maximum ozone concentrations are 74, 65, 51, and 44 ppb in the NOURB-ALL, NOURB-OUT, NOURB-IN, and NOURB-NONE simulations respectively. Similar to the URB-type simulations results, the ozone concentration in the NOURB-ALL simulation is always higher than that in the NOURB-OUT simulation, and the ozone concentration in the NOURB-OUT simulation is always higher than that in the NOURB-IN

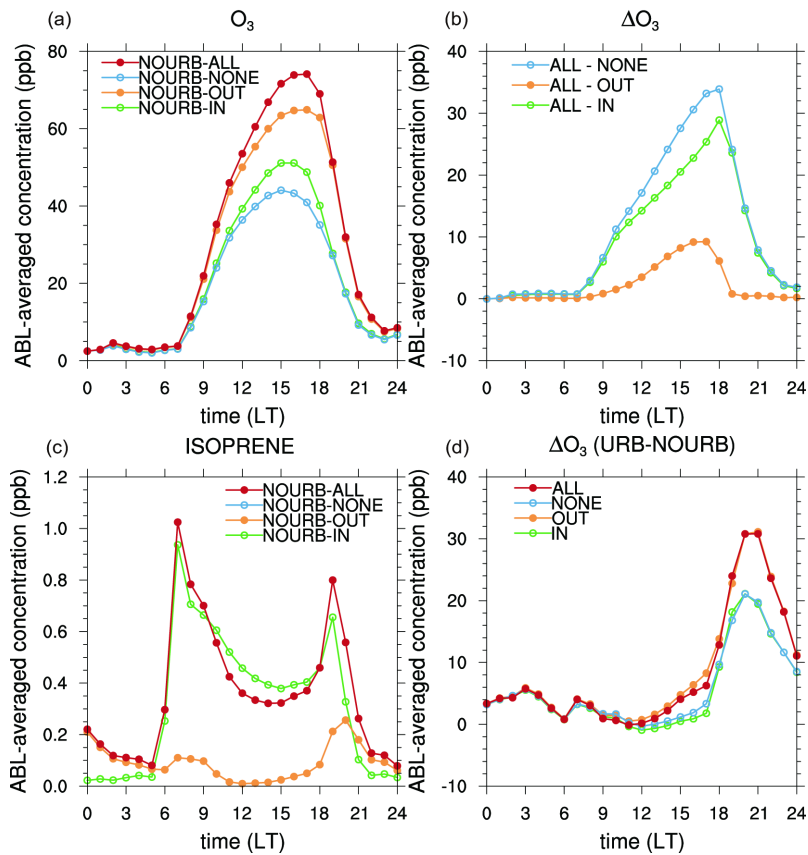


Figure 12. Diurnal variations of atmospheric boundary layer averaged concentrations of (a) ozone, (c) isoprene in the NOURB-ALL, NOURB-OUT, NOURB-IN, and NOURB-NONE simulations. (b) Diurnal variations of atmospheric boundary layer averaged ozone concentration differences between NOURB-ALL simulation and NOURB-OUT, NOURB-IN, or NOURB-NONE simulation in the urban area. (d) Diurnal variations of atmospheric boundary layer averaged ozone concentration differences between the URB-type simulations and NOURB-type simulations.

simulation. Unlike in the IN and NONE simulations, the ozone concentrations in the NOURB-IN and NOURB-NONE simulations are largely perturbed in the afternoon (from 15 to 17 LT). The daily maxima of ozone concentration appear at 17 LT in the NOURB-ALL and NOURB-OUT simulations, which appear one hour earlier than those in the ALL and OUT simulations. The times of daily maxima of ozone concentration in the NOURB-IN and NOURB-NONE simulations are the same as those in the IN and NONE simulations, respectively (Fig. 12a). The time differences of daily maxima of ozone concentration are caused by the lack of the urban breeze circulation which transports MA_PAN. On average, the ozone concentration in the NOURB-ALL simulation in the daytime (from 06 to 19 LT) is 3.8, 12.8, and 16.0 ppb higher than in the NOURB-OUT, NOURB-IN, and NOURB-NONE simulations, respectively. In the nighttime, the ozone concentration in the NOURB-ALL simulation is 0.3, 5.0, and 5.3 ppb higher than in the NOURB-OUT, NOURB-IN, and NOURB-NONE simulations, respectively (Fig. 12b). In the daytime and nighttime, the ozone concentration differences between the simulations in the NOURB-type simulations generally decrease. The daily maximum ozone concentration differences between the URB-type simulations and NOURB-type simulations are 30.8, 31.1, 21.1 and 21.1 ppb in the ALL, OUT, IN and NONE

simulations, respectively, and appear at 21 LT (in the ALL and OUT simulation) and 20 LT (in the IN and OUT simulations) (Fig. 12d). These ozone concentration differences between the URB-type simulations and NOURB-type simulations are quite small until 15 LT but dramatically increase as the urban breeze and the sea breeze prevails. Also, the ozone concentration difference between the ALL and NOURB-ALL simulations is almost the same as that between the OUT and NOURB-OUT simulations, and the ozone concentration difference between the IN and NOURB-IN simulations is almost the same as that between the NONE and NOURB-NONE simulations. These results also indicate that the biogenic isoprene emission in the surrounding area is much more important to the ozone concentration in Seoul rather than the biogenic isoprene emission in the urban area.

Unlike ozone, the isoprene concentration in the urban area increases in the NOURB-type simulations. In the NOURB-type simulations, the isoprene concentrations increase rapidly and reach the daily maximum concentrations in the morning. The time of daily maximum is 2 hours earlier than in the URB-type simulations. After that, the isoprene concentrations decrease slowly until the evening, similar to the URB-type simulations. In the evening, the isoprene concentrations slightly (in the

NOURB-OUT simulation) or considerably (in the NOURB-ALL and NOURB-IN simulations) increase. The isoprene concentrations in the NOURB-type simulations are almost two times higher than those in the URB-type simulations. This can be explained by the OH radical. As mentioned above, OH radical converts isoprene to smaller molecules. The OH radical is produced by the photo-dissociation reactions of ozone. In the NOURB-type simulations, the ozone concentrations are generally lower than in the URB-type simulations (Fig. 12d). As a result, the OH radical concentrations in the NOURB-type simulations are 10–20% lower than those in the URB-type simulations (not shown). Therefore, the reaction between OH radical and isoprene is suppressed, and fewer isoprene is converted to smaller molecules in the NOURB-type simulations.

Figure 13 shows the atmospheric boundary layer averaged contributions of individual processes to the ozone concentration in the urban area from 06 to 20 LT in the NOURB-type simulations. Unlike in the URB-type simulations, chemical reactions are not the largest ozone source in the urban area in the afternoon except for the NOURB-ALL simulation. The ozone transport rate is relatively larger than the ozone production rate in the afternoon in the NOURB-OUT, NOURB-IN, and NOURB-NONE simulations (Fig. 13). On average, the ozone production rates are 4.3, 2.0, 1.2, and -0.7

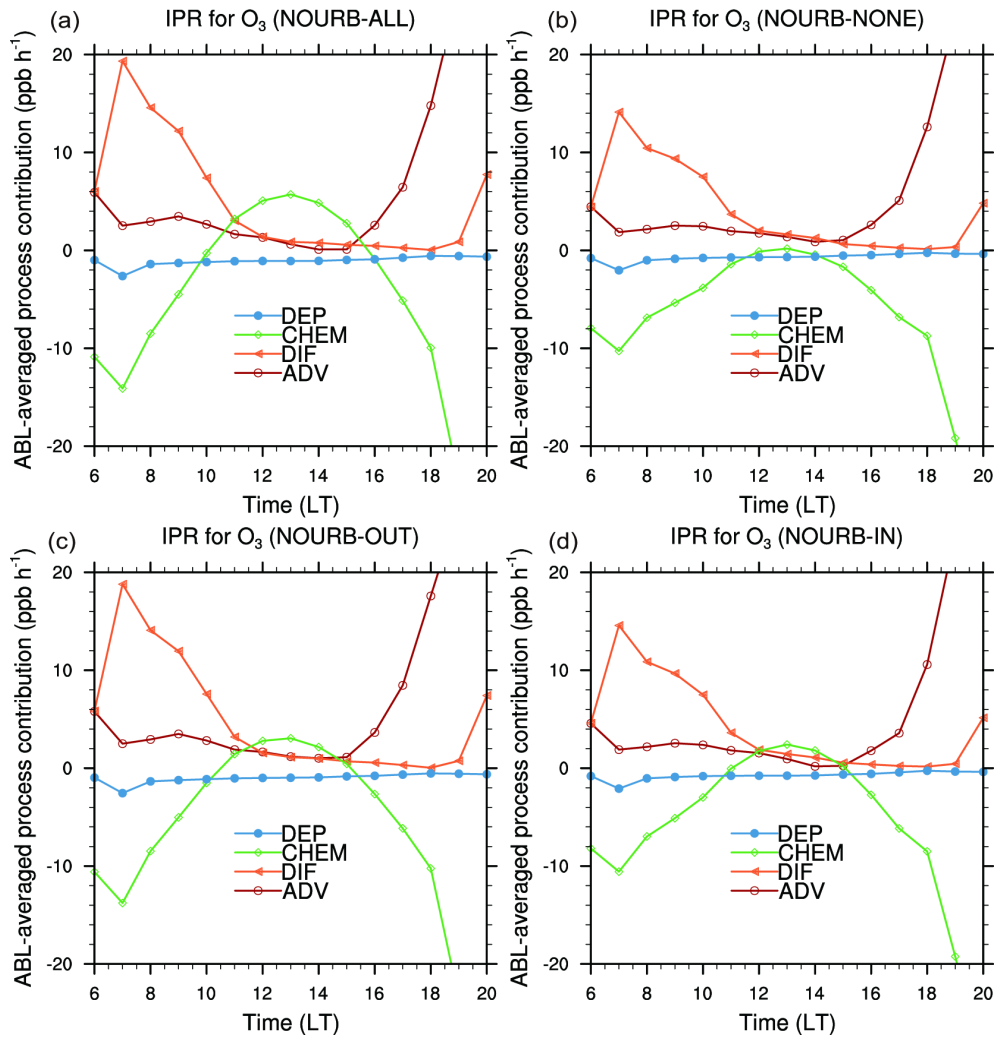


Figure 13. Diurnal variations of atmospheric boundary layer averaged contributions of individual processes to ozone concentration in the (a) NOURB-ALL, (b) NOURB-NONE, (c) NOURB-OUT, and (d) NOURB-IN simulations in the urban area from 06 to 20 LT.

ppb h⁻¹ from 11 to 15 LT in the NOURB-ALL, NOURB-OUT, NOURB-IN, and NOURB-NONE simulations, respectively. In addition, the ozone transport rates are 2.1, 2.9, 2.7, and 3.3 ppb h⁻¹ from 11 to 15 LT in the NOURB-ALL, NOURB-OUT, NOURB-IN, and NOURB-NONE simulations, respectively. It is interesting phenomenon that the urban breeze circulation is weakened, the ozone production rate in the urban area is decreased, and the ozone transport rate is increased.

Weakened urban breeze circulation suppresses the advection of precursors of ozone from the surrounding area into the urban area, and weakened urban heat island depresses the upward motion over the urban area. As a result, the vertical advection of precursors of ozone from the surface into the upper parts of the atmospheric boundary layer is depressed, and the chemical production of ozone is also suppressed. That is the reason why the concentration difference between the urban area and the surrounding area is increased and more ozone is transported from the surrounding area to the urban area (Figs. 5 and 13).

The MA_PAN concentration and the contributions of individual processes to the MA_PAN concentration in the NOURB-type simulations are shown in Figs. 14 and 15, respectively. In the NOURB-ALL and NOURB-OUT simulations, the MA_PAN concentrations generally decrease,

especially in the forenoon and nighttime, compared to the ALL and OUT simulations. However, the MA_PAN concentrations in the daybreak and afternoon are increased (Fig. 14a). The MA_PAN concentration decrements in the nighttime are caused by the decrements of the transport of MA_PAN, increments of the dry deposition of MA_PAN, and increments of the chemical decomposition. The MA_PAN concentration increments in the daybreak and afternoon are caused by the decrements of chemical decomposition of MA_PAN. However, in the NOURB-IN simulation, the MA_PAN concentration increases (Fig. 14a and c) compared to the IN simulation. The MA_PAN concentration differences between the NOURB-type simulations are almost the same as those between the URB-type simulations (Fig. 14b). The daily maxima of MA_PAN concentration appear at 16 LT in the NOURB-ALL simulation, which is one hour earlier than in the ALL simulation like ozone.

In the NOURB-OUT simulation, MA_PAN is transported from the surrounding area into the urban area, similar to the OUT simulation (Fig. 15c). The amount of transport of MA_PAN in the NOURB-OUT simulation is slightly smaller than that in the OUT simulation in the daytime, but the ratio between advection and diffusion is different. In the NOURB-OUT simulation, because of weakened urban breeze circulation, the relative

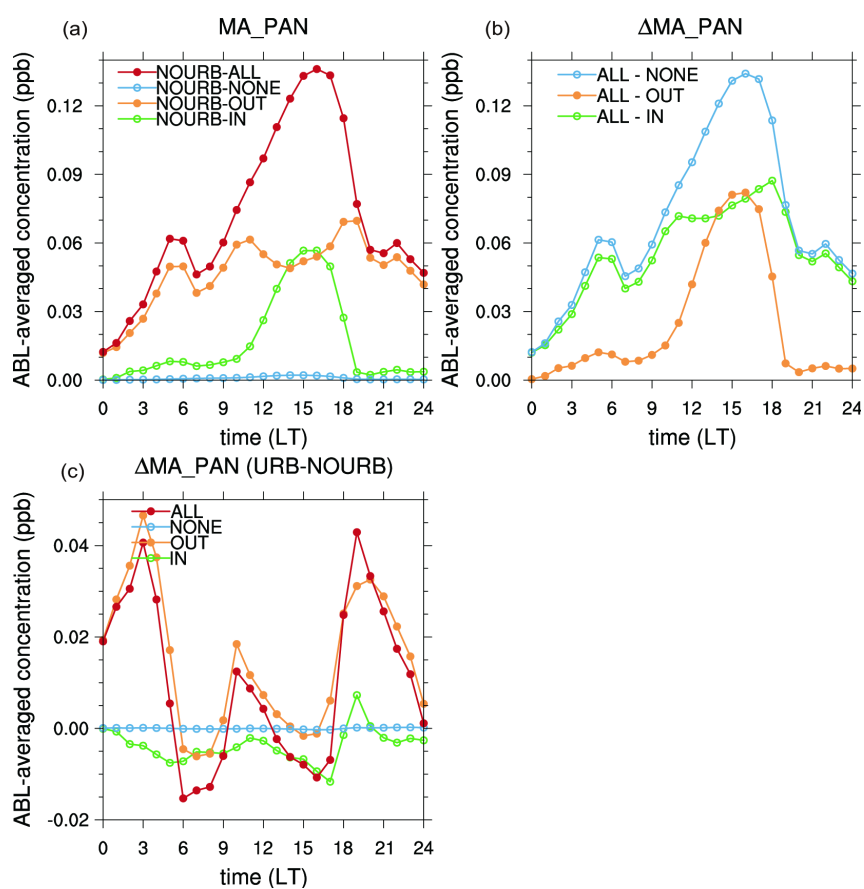


Figure 14. (a) Diurnal variations of atmospheric boundary layer averaged MA_PAN concentration in the NOURB-ALL, NOURB-OUT, NOURB-IN, and NOURB-NONE simulations in the urban area. (b) Diurnal variations of atmospheric boundary layer averaged MA_PAN concentration differences between NOURB-ALL simulation and NOURB-OUT, NOURB-IN, or NOURB-NONE simulation in the urban area. (c) Diurnal variations of atmospheric boundary layer averaged MA_PAN concentration differences between the NOURB-type and URB-type simulations in the urban area.

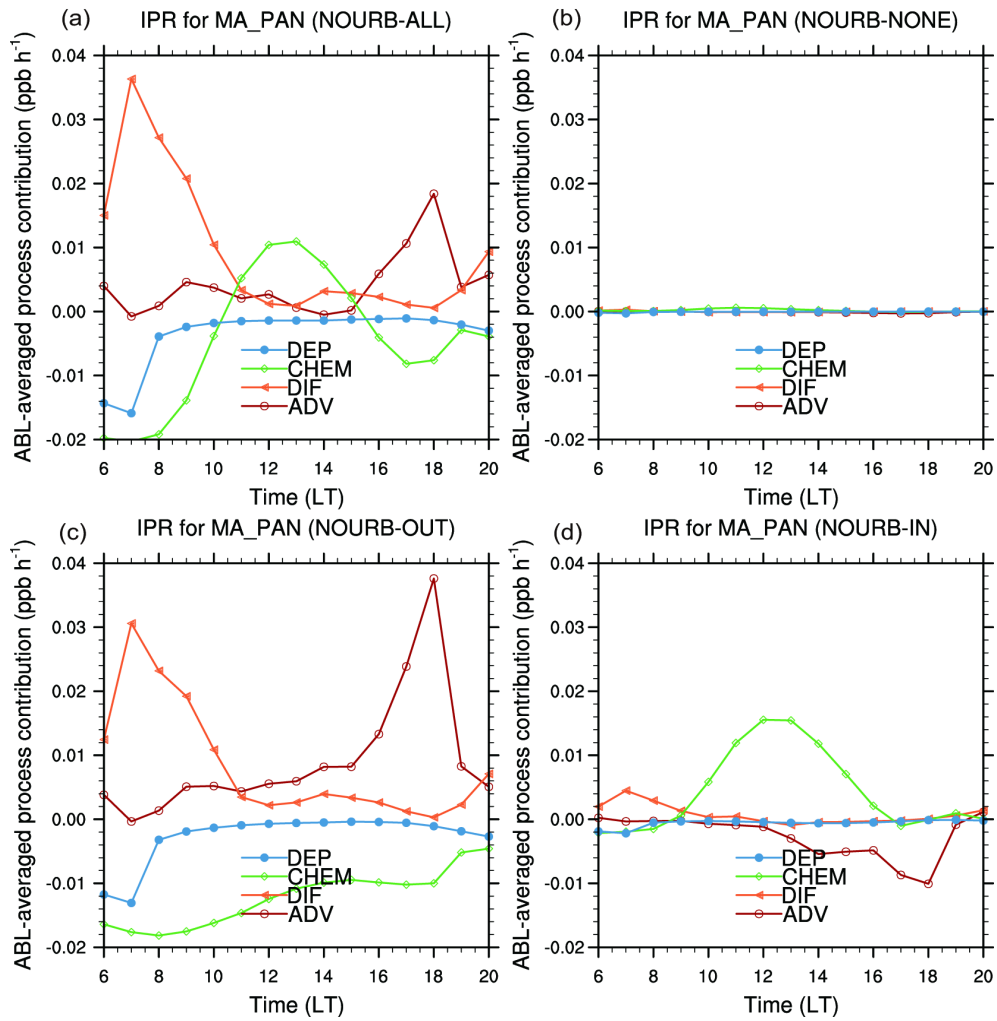


Figure 15. Diurnal variations of atmospheric boundary layer averaged contributions of individual processes to the MA_PAN concentration in the (a) NOURB-ALL, (b) NOURB-NONE, (c) NOURB-OUT, and (d) NOURB-IN simulations in the urban area from 06 to 20 LT.

importance of the advection process to the transport decreases. However, the relative importance of the diffusion process to the transport increases because of the decrement of the advection process and the increment of the diffusion process. It is because the MA_PAN concentration difference between the surrounding area and the urban area increases in the NOURB-OUT simulation. In the NOURB-ALL and NOURB-OUT simulations, the maxima of MA_PAN advection appear at 18 LT, one hour later than in the ALL and OUT simulations (Fig. 15a, c). In the NOURB-IN simulation, MA_PAN is produced in the urban area and is transported from the urban area into the surrounding area similar to the IN simulation, but maxima of transport of MA_PAN appear at 18 LT, not at 16 LT.

4. Summary and conclusions

In this study, the impacts of biogenic isoprene emission on ozone air quality and the effect of interaction between biogenic isoprene emission and urban breeze circulation on ozone air quality in the Seoul metropolitan area were examined using numerical models. On average, the daily maximum of

ozone concentration increases by 37 ppb due to the biogenic isoprene emission. The biogenic isoprene emission in the surrounding area largely influences ozone concentration in the urban area rather than the biogenic isoprene emission in the urban area. Also, the biogenic isoprene emission in the surrounding area changes the diurnal variation of ozone concentration in the urban area. It retards the time of daily maximum of ozone concentration from 15 to 18 LT. Even though the ozone concentration in the surrounding area is higher than that in the urban area and the urban breeze circulation is well developed, the contribution of the transport of ozone is smaller than the contribution of chemical reactions of ozone in the daytime. Although the biogenic isoprene emission only exists in the surrounding area, the contribution of the chemical production of ozone in the urban area is larger than the contribution of the transport of ozone in the urban area. It is due to the precursors of the ozone, which are produced from the biogenic isoprene emission in the surrounding area, transport from the surrounding area into the urban area and produce ozone in the urban area by chemical reactions between NO_x .

Even though the impacts of the biogenic isoprene emission on the ozone concentration is well known, how the biogenic isoprene emission affects the ozone concentration in the urban area is not well understood. In

this study, we found that MA_PAN is transported from the surrounding area into the urban area and affects ozone concentration in the urban area. Also, the daily maxima of MA_PAN transportation appear in the late afternoon when the urban breeze circulation is well developed. Other species such as formaldehyde are negligibly transported from the surrounding area into the urban area.

Urban breeze circulation affects ozone concentration in the urban area. When the urban breeze circulation is weakened, the ozone concentrations decrease especially when the biogenic isoprene emission in the surrounding area exists (NOURB-ALL and NOURB-OUT simulations). Furthermore, the diurnal variations of ozone concentration also change especially when the biogenic isoprene emission in the surrounding area is absent. It is quite interesting that when the urban breeze circulation is weakened, the contributions of the transport process to the ozone concentration in the urban area increase. However, the contributions of chemical reactions to the ozone concentration in the urban area decrease. These features are caused by the decrement of the transports of the precursors of ozone from the surrounding area into the urban area. As a consequence, ozone concentration difference between the urban area and surrounding area increases and then more ozone is transported from the surrounding area into the urban area.

This study demonstrates that the biogenic isoprene emission increases ozone concentration in the urban area, especially due to the biogenic isoprene emission in the surrounding area when the synoptic forcing is sufficiently weak. Also, the interaction between the biogenic isoprene emission and the urban breeze circulation increases ozone concentration in the urban area. The results presented in this study suggest that forests in and near the urban area influence air quality significantly under a proper synoptic condition.

References

- Bao, H., Kondo, A., Kaga, A., Tada, M., Sakaguti, K., Inoue, Y. Shimoda, Y., Narumi, D., and Machimura T.: Biogenic volatile organic compound emission potential of forests and paddy fields in the Kinki region of Japan, *Environ. Res.*, 106, 156–169, 2008.
- Bao, H., Shrestha, K. L., Kondo, A., Kaga, A., and Inoue, Y.: Modeling the influence of biogenic volatile organic compound emissions on ozone concentration in summer season in the Kinki region of Japan, *Atmos. Environ.*, 44, 421–431, 2010.
- Carslaw, N., Bell, N., Lewis, A. C., McQuaid, J. B., and Pilling, M. J.: A detailed case study of isoprene chemistry in the EASE96 Mace Head campaign, *Atmos. Environ.*, 34, 2827–2836, 2000.
- Carter, W. P. L.: Documentation of the SAPRC-99 chemical mechanism for VOC reactivity assessment, Final Report to California Air Resources Board, Contract No. 92-329 and 95-308, Air Pollution Research Center and College of Engineering Center for Environmental Research and Technology, University of California Riverside, California, 2000.

- Chameides, W. L., Lindsay, R. W., Richardson, J., and Kiang, C. S.: The role of biogenic hydrocarbons in urban photochemical smog: Atlanta as a case study, *Science*, 241, 1473–1475, 1988.
- Foley, K. M., Roselle, S. J., Appel, K. W., Bhave, P. V., Pleim, J. E., Otte, T. L., Mathur, R., Sarwar, G., Young, J. O., Gilliam, R. C., Nolte, C. G., Kelly, J. T., Gilliland, A. B., and Bash, J. O.: Incremental testing of the community multiscale air quality (CMAQ) modeling system version 4.7, *Geosci. Model Dev.*, 3, 205–226, 2010.
- Geng, F., Tie, X., Guenther, A., Li, G., Cao, J., and Harley, P.: Effect of isoprene emissions from major forests on ozone formation in the city of Shanghai, China, *Atmos. Chem. Phys.*, 11, 10449–10459, 2011.
- Guenther, A. B., Zimmerman P. R., Harley, P. C., Monson, R. K., and Fall R.: Isoprene and monoterpene emission rate variability: Model evaluations and sensitivity analyses, *J. Geophys. Res.*, 98, 12609–12617, 1993.
- Guenther, A., Hewitt, C. N., Erickson, D., Fall, R., Geron, C., Graedel, T., Harley, P., Klinger, L., Lerdau, M., Mckay, W. A., Pierce, T., Scholes, B., Steinbrecher, R., Tallamraju, R., Taylor, J., and

- Zimmerman, P.: A global model of natural volatile organic compound emissions, *J. Geophys. Res.*, 100, 8873–8892, 1995.
- Guenther, A., Karl, T., Harley, P., Wiedinmyer, C., Palmer, P. I., and Geron, C.: Estimates of global terrestrial isoprene emissions using MEGAN (Model of Emissions of Gases and Aerosols from Nature), *Atmos. Chem. Phys.*, 6, 3181–3210, 2006.
- Haagen-smith, A. J., Fox, M. M.: Photochemical ozone formation with hydrocarbons and automobile exhaust, *J. Air Pollut. Control Assoc.*, 4, 105–109, 1954.
- Hellen, H., Tykkä, T., and Hakola, H.: Importance of monoterpenes and isoprene in urban air in northern Europe, *Atmos. Environ.*, 59, 59–66, 2012.
- Houyoux, M. R., Vukovich, J. M., Coats, C. J., Wheeler, N. J. M., and Kasibhatla, P. S.: Emission inventory development and processing for the seasonal model for regional air quality (SMRAQ) project, *J. Geophys. Res.*, 105, 9079–9090, 2000.
- Kim, H. H.: Urban heat island, *Int. J. Remote Sensing*, 12, 2319–2336, 1992.
- Lee, D. S., Holland, M. R., and Falla, N.: The potential impact of ozone on materials in the U. K., *Atmos. Environ.*, 30, 1053–1065, 1996.

- Li, G., Zhang, R., Fan, J., and Tie, X.: Impacts of biogenic emissions on photochemical ozone production in Houston, Texas, *J. Geophys. Res.*, 112, D10309, 2007.
- Lin, S., Liu, X., Le, L. H., and Hwang, S.-A.: Chronic exposure to ambient ozone and asthma hospital admissions among children, *Environ. Health Perspect.*, 166, 1725–1730, 2008.
- McDonnell, W. F., Abbey, D. E., Nishino, N., and Lebowitz, M. D.: Long-term ambient ozone concentration and the incidence of asthma in nonsmoking adults: the ahsmog study, *Environ. Res. Sect. A.*, 80, 110–121, 1999.
- Milford, J. B., Russell, A. G., and McRae, G. J.: A new approach to photochemical pollution control: implications of spatial patterns in pollutant responses to reductions in nitrogen oxides and reactive organic gas emission, *Environ. Sci. Tech*, 23, 1290–1301, 1989.
- Milford, J. B., Gao, D., Sillman, S., Blossey, P., and Russell, A. G.: Total reactive nitrogen (NO_y) as an indicator of the sensitivity of ozone to reductions in hydrocarbon and NO_x emissions, *J. Geophys. Res.*, 99, 3533–3542, 1994.
- Nguyen, H. T., Kim, K.-H., Kim, M.-J.: Volatile organic compounds at an urban monitoring station in Korea, *J. Hazard. Mater.*, 161, 163–

174, 2009.

Pierce, T., Geron, C., Bender, L., Dennis, R., Tonnesen, G., and Guenther, A.: Influence of increased isoprene emissions on regional ozone modeling, *J. Geophys. Res.*, 103, 25611–15629, 1998.

Pleim, J. E.: A combined local and nonlocal closure model for the atmospheric boundary layer. Part I: model description and testing, *J. Appl. Meteorol. Climatol.*, 46, 1383–1395, 2007.

Ryu, Y.-H., Baik, J.-J., and Lee, S.-H.: A new single-layer urban canopy model for use in mesoscale atmospheric models, *J. Appl. Meteorol. Climatol.*, 50, 1773–1794, 2011.

Ryu, Y.-H., Baik, J.-J., Kwak, K.-H., Kim, S., and Moon, N.: Impacts of urban land–surface forcing on ozone air quality in the Seoul metropolitan area, *Atmos. Chem. Phys.*, 13, 2177–2194, 2013.

Ryu, Y.-H., and Baik, J.-J.: Daytime local circulation and their interactions in the Seoul metropolitan area, *J. Appl. Meteorol. Climatol.*, 52, 784–801, 2013.

Sillman, S.: The reaction between ozone, NO_x, and hydrocarbons in urban and polluted rural environment, *Atmos. Environ.*, 33, 1821–1845, 1999.

- Skamarock, W. C., Klemp, J. B., Dudhia, J., Gill, D. O., Barker, D. M., Duda, M. G., Huang, X.-Y., Wang, W., and Powers, J. G.: A description of advanced research WRF version 3, NCAR Tech. Note NCAR/TN-475+STR, 2008.
- Trahan, N. A., and Peterson, C. M.: Factors impacting the health of roadside vegetation, Colorado department of transportation research branch, Final report NO. CDOT-DTD-R-2005-12, 2007.
- Trainer, M., Williams, E. J., Parrish, D. D., Buhr, M. P., Allwine, E. J., Westberg, H. H., Fehsenfeld, F. C., and Liu, S. C.: Models and observations of the impact of natural hydrocarbons on rural ozone, *Nature*, 329, 705-707, 1987.
- USEPA: Guideline for regulatory application of the urban air shed model, US EPA report NO. EPA-450/4-91-013, Office of Air Quality Planning and Standards Technical Support Division, Research Triangle Park, North Carolina, USA, 1991.
- Vogel, B., Fiedler, F., Vogel, H.: Influence of topography and biogenic volatile organic compounds emission in the state of Baden-Württemberg on ozone concentrations in episodes of high air temperatures, *J. Geophys. Res.*, 100, 22907-22928, 1995.
- Williams, J., Roberts, J. M., Fehsenfeld, F. C., Bertman, S. B., Buhr, M. P.,

- Goldan, P. D., Hübler, G., Kuster, W. C., Ryerson, T. B., Trainer, M., and Young, V.: Regional ozone from biogenic hydrocarbons deduced from airborne measurements of PAN, PPN, and MPAN, *Geophys. Res. Lett.*, 24, 1099–1102, 1997.
- Wong, K. K., Dirks, R. A.: Mesoscale perturbations on airflow in the urban mixing layer, *J. Appl. Meteorol.*, 17, 677–688, 1978.
- World Health Organization (WHO): Health aspects of air pollution with particulate matter, ozone and nitrogen dioxide, Report on a WHO working group; Bonn, Germany, 13–15 January 2003, available at: www.euro.who.int/document/e79097.pdf, 2003.
- Yamartino, R. J.: Nonnegative, conserved scalar transport using grid-cell-centered, spectrally constrained blackman cubics for applications on a variable-thickness mesh, *Mon. Weather Rev.*, 121, 753–763, 1993.

초록

자연 발생 이소프렌 배출이 서울 지역 오존 대기질에 미치는 영향

이 광연

지구환경과학부

석사과정

서울대학교

본 연구에서는 중관 강제력이 약할 때 자연 발생 이소프렌 배출이 서울 지역 오존 대기질에 미치는 영향과 자연 발생 이소프렌 배출과 도시풍의 상호작용이 서울 지역 오존 대기질에 미치는 영향을 서울대학교 도시 캐노피 모형과 결합된 WRF 모형과 CMAQ 모형을 이용하여 연구하였다. 자연 발생 이소프렌 배출은 도시 지역의 일 최고 오존 농도를 37 ppb 증가시키며, 서울 지역에서 배출된 자연 발생 이소프렌보다 주변 지역에서 배출된 자연 발생 이소프렌이 도시의 오존 농도에 더 큰 영향을 준다. 도시풍이 잘 발달하고 자연 발생 이소프렌 배출이 있는 경우 낮 동안에는 화학 반응이 오존 농도에 가장 큰 영향을 준다. 이소프렌의 대기 중 체류 시간은 도시의 오존 농도에 직접적으로 영향을 줄 만큼 충분히 길지 않다. 따라서 이소프렌 대신 이소프렌으로부터 생성되는

MA_PAN이 주변 지역에서 배출된 자연 발생 이소프렌과 도시의 오존 사이를 연결시켜준다. 주변 지역에서 생성된 MA_PAN은 도시로 수송되어 오존을 만드는 다른 물질들로 분해된다. 도시풍은 도시의 오존 농도에 영향을 주는 중요한 기상 현상 중 하나다. 도시 지역과 공업 지역 토지 피복이 농경 지역으로 대체된 경우 도시풍은 뚜렷이 발달하지 않는다. 도시풍이 약해짐에 따라 도시 내부의 오존 농도는 전반적으로 약 10% 낮아지며 화학 반응이 도시의 오존 농도에 미치는 영향 또한 낮아진다. 이것은 주변 지역에서 도시로 유입되는 오존 전구체의 양이 줄어들기 때문에 발생한다. 본 연구 결과는 자연 발생 이소프렌이 도시의 오존 농도에 어떻게 영향을 미치는지에 대해 알려준다.

주요어 : 자연 발생 이소프렌 배출, 오존 대기질, 도시 지역, 도시풍 순환, WRF 모형, CMAQ 모형

학번 : 2011-23267

감사의 글

학교에 입학한지 엇그제 같은데 어느덧 석사과정 2년의 시간을 거쳐 졸업을 하게 되었습니다. 그동안 제게 많은 것을 알려주시고 많은 도움을 주신 모든 분들께 감사의 말씀을 드립니다.

먼저 학부부터 지금까지 제게 많은 것을 알려주시고 석사과정동안 부족한 저를 지도해 주신 백종진 교수님께 진심으로 감사드립니다. 또한 바쁘신 와중에 제 논문 심사 위원장을 맡아주신 박록진 교수님과 제 논문 심사위원을 맡아주신 윤순창 교수님께도 깊은 감사를 드립니다.

석사과정동안 저에게 많은 도움과 격려를 준 대류/도시 기상 연구실의 선배, 후배님들께 감사드립니다. 같이 오래있지 않았지만 편히 대해주신 지영 누나, 이것저것 많이 알려주신 승부 형, 연구의 시작에 큰 도움을 주신 영희 누나, 저한테 많은 것을 알려주시고 항상 저 때문에 고생하시는 경환이형, 항상 좋은 조언을 아끼지 않고 해주신 현호 형, 성실하게 항상 연구를 하는 Gana, 같이 수업 들으며 큰 도움을 주신 재명이 형, 대학원 생활동안 같이 지내며 좋은 친구가 되어준 소라누나, 이제 막 연구를 시작하려는 범순이와 새로 들어온 민유에게 깊은 감사를 드립니다. 석사 과정을 같이 지내며 큰 힘이 되어준 승규 형, 진수 형, 정화 누나, 훈영이 형, 민섭이 형, 상무 형, 상원이 형, 재창이 형, 민진

누나, 지원 누나, 지연 누나, 평화 누나, Rijana에게 감사를 드리며 앞으로
로도 각자 하고자 하는 바를 모두 이루시며 계속 함께 하길 바랍니다.

학부부터 대학원 까지 같은 길을 걷고 있는 다솔, 승언, 정우, 병
권, 재희와 같은 길은 아니지만 대학원에 와 있는 민호, 수환, 석영, 도
현에게 감사하며 앞으로 좋은 과학자가 되어 함께하기를 바랍니다.

같이 수업 들으며 공부한 대학원 선, 후배님들과 학부를 같이 보
내고 여기저기 활발하게 진출하고 있는 학부 동기들, 그리고 어렸을 때
부터 함께 해왔던 여러 친구들 모두에게 깊은 감사를 드립니다.

못난 말썽쟁이 아들을 지금까지 키워주신 존경하는 어머니, 아버
지께 애정을 담아 깊은 감사를 드립니다. 때로는 친구처럼 지내는 지금
군복무 중인 동생에게도 깊은 감사를 드립니다. 앞으로도 항상 행복과
행운이 우리가족과 함께하기를 바랍니다.

마지막으로 지금 이 글을 읽어주신 분께 감사드립니다. 항상 하는
일마다 행복한 결과를 얻으시기를 바랍니다.